# The role of STAMP2 in the regulation of autophagy in prostate cancer cells

Matthew Ng Yoke Wui

Thesis for the Master of Science degree
in Molecular Biosciences

Department of Biosciences
The Faculty of Mathematics and Natural Sciences

UNIVERSITY OF OSLO

June 2017

*The role of STAMP2 in the regulation of autophagy in prostate cancer cells*

Matthew Ng Yoke Wui

# Acknowledgements

The work described here was carried out in the Department of Biosciences, Faculty of Mathematics and Natural Sciences, University of Oslo, in the lab of Fahri Saatcioglu in the period of June 2015 to July 2017.

To my supervisor Fahri Saatcioglu, I owe my sincerest gratitude for providing me with a wonderful opportunity to grow as a researcher. Your passion for science has been an inspiration to me ever since the first lecture of MBV3090. I appreciate the trust that you had in me and for giving me the freedom to be curious and to make mistakes, many mistakes. Thank you for helping me grow both as a person and as a researcher.

I would also like to extend my appreciation to my co-supervisor Yang Jin for the excellent mentoring that he has provided. Your patience has been as limitless as my questions.

Thanks to the FS lab family, who have made the lab feel like a home away from home. It has truly been a great pleasure to work alongside a group of people who are not only talented scientists but also great friends.

I am grateful to Professor Anne Simonsen and members of the Simonsen lab for kindling my interest in autophagy, and for all of the invaluable scientific and not so scientific discussions.

To my family and friends, thank you for the support you have provided me throughout my education and for showing me that there is life beyond the lab bench.

Many thanks,

Matthew Ng

Oslo, May 2017

# Summary

In the past decades, the role of autophagy in cancer biology has entered the spotlight. The dependence of tumors on the lysosomal degradation pathway has opened up exciting new avenues for precise targeted cancer therapies. In prostate cancer (PCa), the inhibition of autophagy interferes with tumor growth and may sensitize them to treatments such as androgen ablation therapy. Here, we focus on the potential role that the androgen regulated protein Six Transmembrane Protein of Prostate 2 (STAMP2) plays in regulating autophagy in PCa. Attenuating STAMP2 levels in PCa cells leads to increased autophagic flux as evidenced by the increase in long-lived protein degradation, microtubule-associated protein 1A/1B-light chain 3 (LC3) lipidation and characteristic intracellular puncta formation. This repressive regulation appears to be, in part, post-translationally regulated through Unc-51-Like kinase 1 (ULK1) phosphorylation and transcriptionally modulated by upregulation of autophagy related genes. Similarly, gene expression analysis in a cohort of 499 primary PCa tumors has shown that STAMP2 and LC3 family mRNA expression are inversely correlated with each other. Among the group of upregulated genes are the target genes for transcription factor EB (TFEB), a master regulator of lysosomal biogenesis. Consistently, TFEB nuclear translocation was increased upon STAMP2 knockdown, suggesting that it is activated to transcribe target genes. Consequently, lysosomal number was increased upon STAMP2 depletion, supporting TFEB activation. In summary, these data show that STAMP2 represses autophagy in PCa by modulation of ULK1 phosphorylation and TFEB activity.

# Abbreviations

| | |
|---|---|
| **ADT** (Androgen deprivation therapy) | **LC3** (Microtubule-associated proteins 1A/1B-light chain 3) |
| **AKT** (Protein kinase B) | **LNCaP** (Lymph node carcinoma of the prostate) |
| **AMPK** (5' adenosine monophosphate-activated protein kinase) | **mAB** (Monoclonal antibody) |
| **AR** (Androgen receptor) | **mTOR** (Mammalian target of rapamycin) |
| **ATF4** (Activating transcription factor 4) | **NF-κB** (Nuclear factor kappa B) |
| **Atg** (AuTophaGy related) | **PCa** (Prostate cancer) |
| **BafA1** (Bafilomycin A1) | **PE** (Phosphatidyl ethanolamine) |
| **BCa** (Breast Cancer) | **PI3K** (Phosphatidylinositol-3 kinase) |
| **CRPC** (Castration resistant prostate cancer) | **PIN** (Prostate intraepithelial neoplasia) |
| **DHT** (Dihydrotestesterone) | **PSA** (Prostate Specific Antigen) |
| **E1** (Ubiquitin-activating enzyme) | **PTEN** (Phosphatase and tensin homologue deleted on chromosome ten) |
| **E2** (Ubiquitin-conjugating enzyme) | **R1881** (Synthetic androgen) |
| **ER** (Endoplasmic reticulum) | **ROS** (Reactive oxygen species) |
| **E2R** (Estrogen receptor) | **RT-PCR** (Real-time quantitative polymerase chain reaction) |
| **FAD** (Flavine adenine dinucleotide) | **siRNA** (Short interfering RNA) |
| **FAK** (Focal adhesion kinase) | **STAMP** (Six transmembrane protein of the prostate) |
| **GABARAP** (Gamma-aminobutyric acid receptor-associated protein) | **TFEB** (Transcription factor EB) |
| **GAPDH** (Glycerophosphate dehydrogenase) | **TNFα** (Tumor necrosis factor alpha) |
| **IF** (Immunofluorescence) | **ULK** (Unc-51-Like kinase) |
| **IL** (Interleukin) | **UPR** (Unfolded protein response) |

# Contents

# 1 General Introduction

## 1.1 Prostate Cancer

### 1.1.1 The prostate

The prostate is a muscular mammalian reproductive gland which in humans is usually the size of a walnut and is located within the pelvic region, below the bladder and surrounding the urethra (1). Its purpose is to secrete a slightly alkaline fluid to aid sperm cells by promoting their viability and motility (2). A typical human adult prostate epithelium is composed of at least three different cell types, tall columnar luminal cells, basal cells and a small population of neuroendocrine cells. The luminal cells secrete Prostate Specific Antigen (PSA), are androgen receptor (AR) positive, and rely on androgens for their survival. The basal cells that lie between the basement membrane and the luminal cells express low levels of AR and are not dependent on androgen signaling for their survival. Similar to basal cells, a small population of neuroendocrine cells express little to no AR and are androgen-independent (1). Neuroendocrine cells are found in the basal cell compartment and express neuroendocrine markers, such as Chromogranin A and neuron specific enolase (3). The prostate is enveloped by a stroma that is made up of nerve cells, smooth muscle, fibroblasts and lymphatic cells and consists of three zones: 1) The peripheral zone which is the area closest to the rectum, makes up approximately 75% of the prostate. This zone is therefore the most easily identified during a digital rectal examination 2) The transition zone which is found in between the peripheral and central zone. The transition zone of the prostate enlarges as men age, eventually outgrowing the peripheral zone to form benign prostatic hyperplasia (BPH). 3) The central zone which is the one that is furthest away from the rectum (4, 5).

### 1.1.2 Prostate cancer epidemiology

PCa is the most frequently diagnosed cancer in North America, second only to skin cancer (6), and is the second leading cause of death among males (7). In Norway, PCa represents the highest diagnosed cancer type in males with 5061 new cases reported in 2015 and makes up 15.8 % of the 156414 cancer incidences reported between the period of 2011-2015 (8). PCa incidences have been on the rise in the past decades and are attributed to the advent of improved PCa diagnostics such as Prostate Specific Antigen (PSA) screening (9, 10). Interestingly, the

survival rate is higher in the United States and Northern Europe and is believed to be the consequence of improved detection of latent tumors (11).

The predisposition to prostate carcinogenesis is governed by multiple risk factors, such as age, diet and smoking. PCa is generally a disease of aging, whereby three quarters of PCa incidences were diagnosed in men over 65 years old (11). Racial descent is an additional risk factor with the highest rates of incidence and mortality of PCa in the United States of America occurring in African-American males (12). Obesity and excessive intake of dietary fat is associated with increased susceptibility of developing PCa (13, 14). Other environmental factors, such as lack of exercise and smoking are additional important risk factors. Heavy cigarette smokers carry a 30% increased chance of PCa mortality compared to their non-smoking counterparts (15).

## 1.1.3 Prostate carcinogenesis

The progression of a normal prostate to an aggressive hormone-refractory prostatic adenocarcinoma is a complex process involving multiple genetic and epigenetic transformations that are yet to be fully understood. The initial detectable morphological change is the development of pre-cancerous Prostatic Intraepithelial Neoplasia (PIN). PIN are characterized by increased cellular proliferation, luminal epithelial growth, disruption of the basal cell layer, variations in DNA content and increased nuclear variation (16). Androgen deprivation therapy (ADT) significantly reduces the prevalence of PIN suggesting that PIN survival is androgen-dependent (17). PIN are eventually able to develop into PCa that are invasive to the neighboring stroma (18). PCa cells that are able to penetrate the basal membrane to enter the blood or lymphatic circulatory systems to be re-established as micro metastasis at a distant region, most frequently in the bones, brain, liver, lymph nodes or lungs (16).

PCa severity can be classified by staging systems such that standard descriptions are used to communicate the severity of the disease. Staging is based on the results of the prostate biopsy including tumor size, spreading of the cancer, the number of observable tumors, and serum PSA levels. The two most commonly used staging systems are the TNM (T-Primary tumor size and localization; N-Spreading to Lymph Nodes; M-Metastasis) system and Gleason grading (19). This is particularly important with respect to the selection of treatment options and estimating patient survival. Recent profiling of 333 primary prostate carcinomas has shown that 74% of the tumors analyzed belonged to one of seven molecular subtypes. These subtypes are defined

by *ERG* gene fusion, *ETV1*, *ETV4* and *FL1* fusion or overexpression and by mutations in *SPOP*, *FOXA1* and *IDH1* (20).
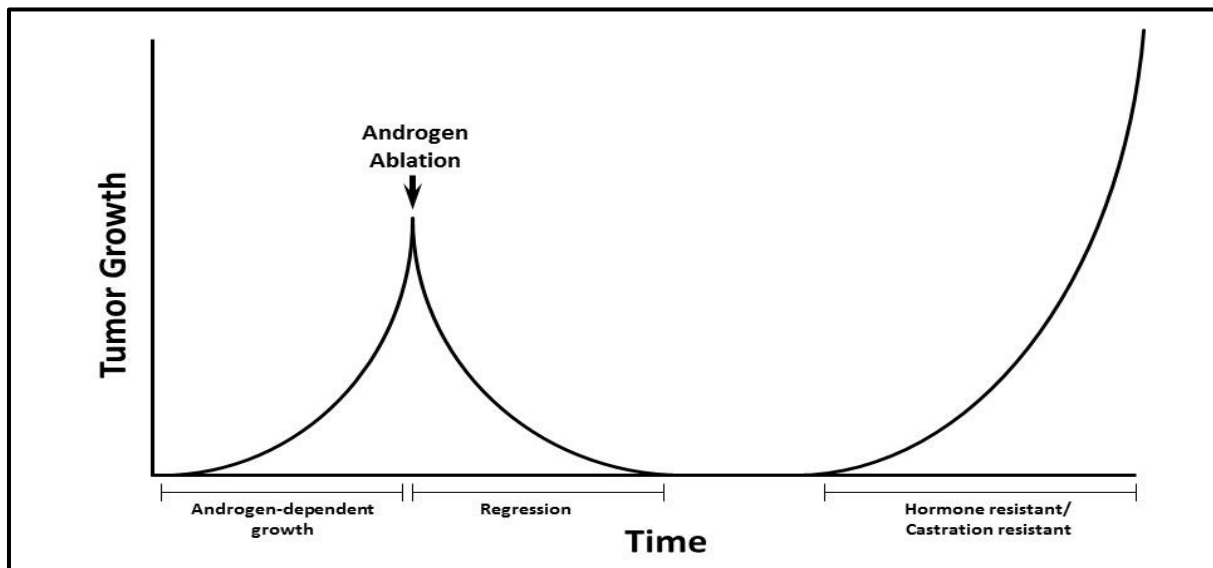


**Figure 1. Prostate cancer progression.** Initial PCa growth is dependent on androgens, which activates and promotes tumor growth and survival. Upon depletion of androgens, the size of the tumor regresses. However, the disease often recurs in the form of castration resistant tumors that no longer responds to the removal of androgens.

The dependence of prostatic tissue on androgen signaling provides an avenue for targeting PCa in the form of ADT. ADT can exist in the form of surgical castration, AR inhibition using AR antagonists such as bicalutamide and preventing testicular and adrenal androgen production using abiraterone or leuprolide. However, despite initial regression of tumor growth after ADT, tumors often relapse as androgen ablation insensitive PCa (Fig. 1). This form of androgen independent PCa is therefore called Castration Resistant Prostate cancer (CRPC). Despite their non-responsiveness to androgen ablation, AR is constantly active in CRPC cells by multiple mechanisms (21). CRPCs are often more aggressive compared to their androgen dependent counterparts and are more prone to metastasis (22).
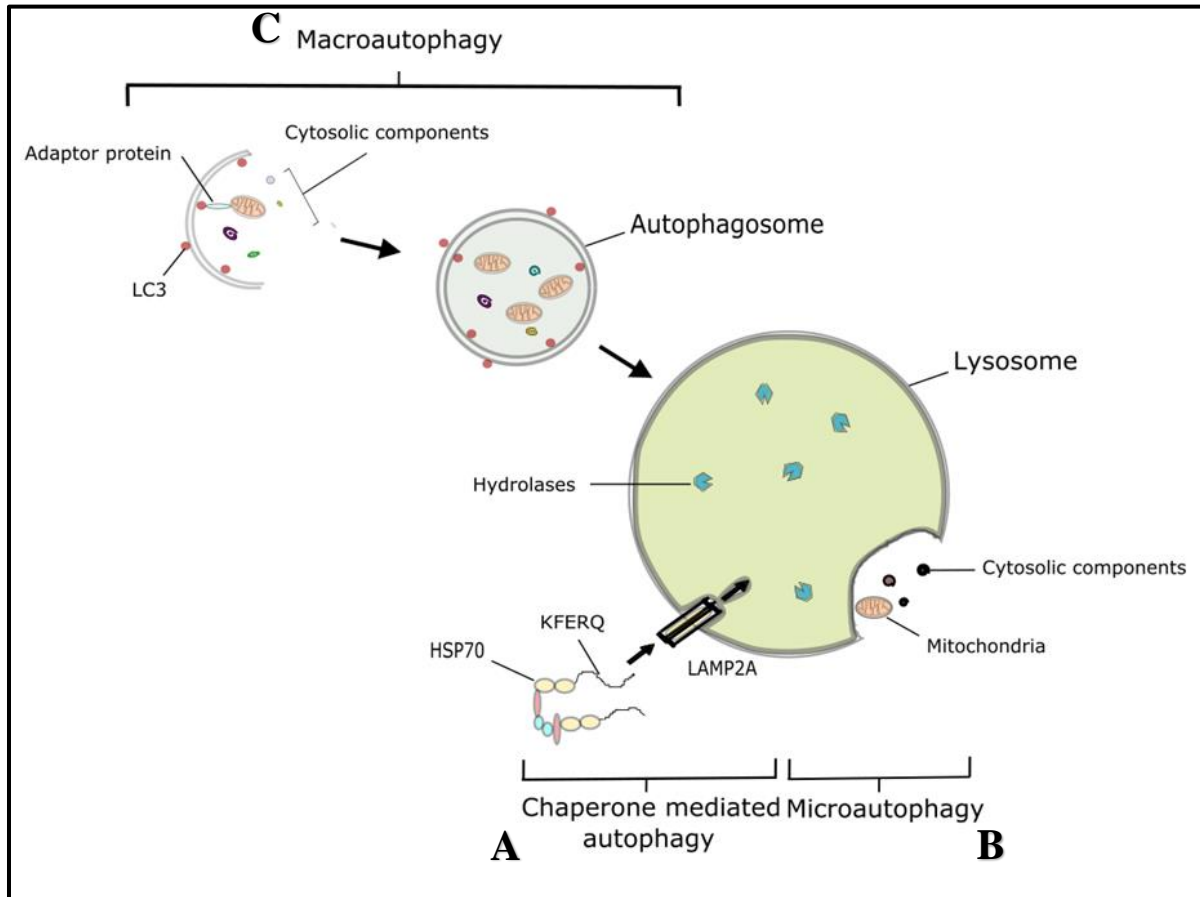
## 1.2 Autophagy

### 1.2.1 Autophagy



**Figure 2. The three main pathways of autophagy. A**. In chaperone-mediated autophagy, cytoplasmic proteins are unfolded and trafficked to the lysosomes by HSC70. The protein is then directly translocated through LAMP2A into the lysosomal lumen. **B**. Cytoplasmic components are engulfed by direct invagination of the lysosomal membrane during microautophagy. **C**. During macroautophagy, the cytosol is enveloped by an initiating phagophore. The phagophore is lined with phosphatidylethanolamine conjugated LC3 to which autophagy adaptor proteins carrying specific cargo are able to bind. The phagophore seals to form an autophagosome that fuses with lysosomes to form an autolysosome, such that hydrolases are able to degrade the contents of the autophagosome. (Figure was adapted from Kaur and Debnath, 2015.)

The Belgian biochemist Christian de Duve won the Nobel Prize in Physiology and Medicine in 1974 for his discovery of the lysosome. This hydrolase filled membrane compartment is the integral endpoint of a complex set of membrane trafficking pathways including one which de Duve termed autophagy. Autophagy, the name being derived from the Greek words auto and phagos meaning self-eating, is a catabolic degradation process whereby cellular components are translocated to lysosomes for their degradation. Autophagy, specifically macroautophagy,

is in essence a membrane trafficking event where the cytosol is sequestered in vesicles and is brought to the lysosomes. There are three main forms of autophagy: Microautophagy, Chaperone Mediated Autophagy (CMA) and Macroautophagy. Microautophagy is the process whereby the lysosomal membrane invaginates and engulfs cytoplasmic components (24). During CMA, soluble cytosolic proteins are delivered directly to lysosomes by heat shock proteins (HSP). Briefly, protein substrates bearing the KFERQ amino acid sequence (25) are unfolded and delivered by HSC70 (26) to the lysosome associated membrane protein type 2A (LAMP2A) which translocates the substrates directly into the lysosomal lumen.

Macroautophagy, henceforth referred to as autophagy for simplicity, involves the formation of a double membrane vesicle that engulfs cytoplasmic components to be shuttled to the lysosome for degradation. This double membrane vesicle, termed the autophagosome, is formed when a phosphatidylinositol-3-phosphate (PI(3)P) rich isolation membrane called the phagophore (27), engulfs cytoplasmic components. The autophagosome then matures by fusion with endosomes to form amphisomes or directly to lysosomes to form autolysosomes for their degradation. The origin of the autophagosomal membrane is not well understood and multiple cellular structures have been implicated in the initial formation of the autophagosome. Various reports suggest that the autophagosomal membrane can be derived from the plasma membrane (28), the mitochondria (29), the Golgi apparatus (30) or, the most likely source, the endoplasmic reticulum (ER) (27).

Selective autophagy mediates the degradation of specific cellular components such as damaged organelles, protein aggregates or internalized pathogens. The specificity of the cargo that is incorporated into the autophagosome is determined by autophagy adaptor proteins. These adaptor proteins contain binding domains for association to their cargo and to LC3 (a ubiquitin-like protein that lines the autophagosme membrane). For example, the autophagic degradation of mitochondria, termed mitophagy, is mediated by both NDP52 and OPTN but not p62 ( also known as SQSTM1) (31). Other forms of selective autophagy include degradation of nuclear material (nucleophagy) (32), lysosomes (lysophagy) (33, 34), peroxisomes (pexophagy) (35), endoplasmic reticulum (ER-phagy) (36), bacteria (xenophagy) (37) and protein aggregates (aggrephagy) (38).
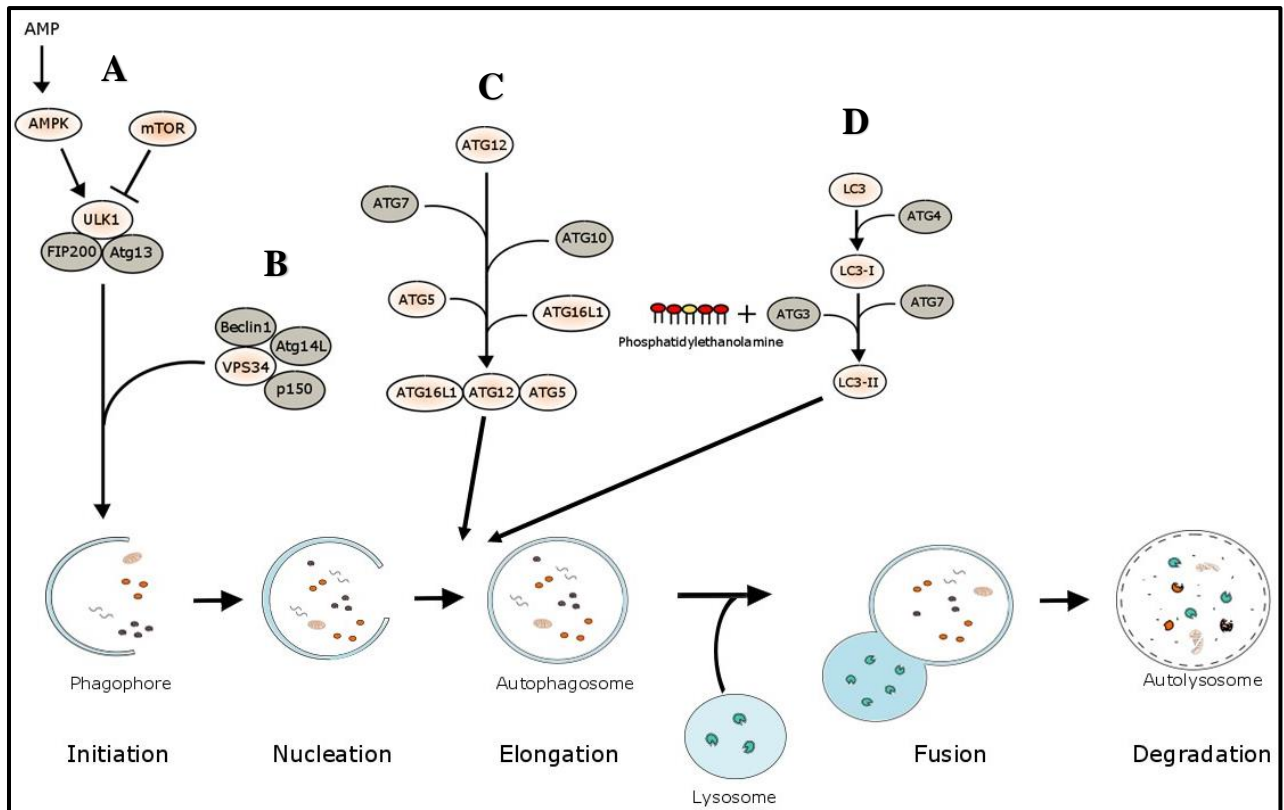
## 1.2.2 Mechanism of autophagy



**Figure 3. The autophagic mechanism.** This figure summarizes the progression and development of the autophagosome. The phagophore membrane elongates and engulfs cytoplasmic components to form an autophagosome. As the autophagosome matures, it fuses with lysosomes and the contents of the autophagosome is degraded by lysosomal hydrolases. Autophagy is dependent on four multi-component complexes: **A**. The ULK complex is made up of ULK1, FIP200 and ATG13 and its formation is regulated by AMPK and mTOR. **B**. The PI3K class-III complex becomes phosphorylated and then generates PI3P that is required for recruitment of autophagy proteins to the phagophore. **C**. The ATG16L1-ATG12-ATG5 conjugate binds directly to membranes and determines the sites of LC3 lipidation. **D**. The ubiquitin like protein, LC3 is first cleaved at the C-terminus by ATG4 and is conjugated to phosphatidyl ethanolamine by ATG7 and ATG3.

The autophagic machinery is driven by the products encoded by autophagy-related (Atg) genes, of which 33 have been identified in humans. The protein products of these Atg genes are necessary in multiple stages of autophagy from autophagosome formation and maturation to autophagosome-lysosome fusion (39). The Atg1/unc51-like kinase (ULK) forms a complex with ATG13 and FIP200 and is necessary for the initiation stages of autophagy, possibly through recruitment of ATG9 to LC3 positive endosomal membranes (40). The ULK kinase complex is recruited to the phagophore nucleation site by the C-terminal early targeting (EAT) domain of ULK (41) and by a cluster of positively charged amino acids at the N-terminal region of ATG13 which associates with phosphatidylinositol 3-phosphate (PI3P) at the omegasome (42). Phosphoinositol 3-kinase (PI3K) complex activation allows for the generation of a

localized pool of PI3P that is responsible for the recruitment of Atg proteins to the site of autophagosome formation. VPS34 is able to form two distinct PI3K complexes that are involved in different cellular processes. Complex I consists of VPS34, BECLIN1, VPS15 and ATG14L while Complex II is made up of VPS34, BECLIN1, VPS15 and UVRAG. Complex I functions mainly in regulating autophagy while Complex II is involved in the vacuolar protein sorting pathway in yeast (43). These events form the platform for the binding of ATG12-ATG5-ATG16L complex (44). The PI3K complex phosphorylates PI at the 3-position of the inositol ring to form PI3P to recruit PI3P binding proteins such as WIPI2 (45) and DFCP1 (27). These PI3P binding proteins in turn form a platform to recruit other Atg proteins and complexes such as ATG16L (44), which determines the site of LC3 lipidation (46) to the growing phagophore. ATG9 is the only single transmembrane protein that is required for autophagy. Induction of autophagy causes the translocation of ATG9 positive membranes from the Golgi to the recycling endosome where it is found to colocalize with ATG16L (47).

Downstream of the ULK and PI3K complexes, two ubiquitin like protein systems (ATG16L1-ATG12-ATG5 and ATG8/LC3) are activated. ATG12 is activated by the E1 ubiquitin ligase ATG7 and then conjugated to the lysine on Atg5 by the E2-like enzyme ATG10 (48, 49). Following this, the ATG12-ATG5 conjugate associates with membrane bound ATG16L. The ATG16L1-ATG5-ATG12 complex is recruited to the site of phagophore nucleation by the interaction between ATG16L1 and FIP200 (50). ATG16L is also recruited to the phagophore by the WD repeat domain phosphoinositide-interacting protein 2 (WIPI2) (44). The ATG16l-ATG12-ATG5 complex behaves like an E3 ubiquitin ligase that is required for the lipidation of ATG8 to phosphatidyl ethanolamine (PE). The ubiquitin like protein Atg8 is cleaved at the C-terminal by ATG4 to expose a glycine residue which is conjugated to PE by ATG7 and ATG3 (51). While only Atg8 is present in yeast, there are 6 LC3/Atg8 family members in mammals belonging either to the LC3 subfamily (LC3A, LC3B and LC3C) or the GABARAP family (GABARAP, GABARAPL1 and GABARAPL2/GATE16) (52). The ATG16L1-ATG5-ATG12 complex is responsible for the transfer of LC3 from LC3-ATG3 conjugates to PE (53). The autophagosome is lined with lipidated LC3, allowing for autophagy adaptor proteins containing LC3-intracting regions (LIRs) (54) to be recruited to the autophagosomes. Autophagy adaptor proteins such as p62, ALFY and NBR1 contain LIR and specialized domains which allows them to latch onto cargo to be brought to the autophagosome (55). Mutations or loss of these adaptor proteins have been associated with physiological defects such as Huntington's (56) or Parkinson's disease (57).

Once the autophagosome has been fully formed, Atg8 lining the outer membrane of the autophagosome is cleaved off by the action of Atg4 (58). The sealed autophagosome needs to be trafficked to a lysosome for fusion to degrade its contents. Autophagosomes are brought into close vicinity to lysosomes by their association to the microtubule motor protein dynein (59). Autophagosomes and lysosomes are found in many regions of the cell, but are translocated towards the nuclear region where they are in close enough vicinity to fuse (60). STX17, a t-Snare found only on fully enclosed autophagosomes, is able to bind to its subsequent v-Snare on the lysosomal membrane to aid vesicle tethering (61). ATG14L binds to STX17 located on autophagosomes and is required for autophagosome-lysosome fusion (62). Once fused with the lysosomes, the contents of the autophagosomes are degraded by the lysosomal hydrolases and the products of this degradation are released into the cytosol.

## 1.2.3 Regulation of autophagy

Multiple cellular conditions, such as hypoxia, nutrient deprivation, pathogen infection and ER stress regulate autophagy. Autophagy is first and foremost regulated by the nutrient sensing mechanisms of the cell, most notably mammalian target of rapamycin complex 1 (mTORC1) and AMP-activated protein kinase (AMPK) (63). Depletion of vital cellular nutrients such as glucose and amino acids leads to the inactivation of mTORC1 and the increase in cellular adenosine monophosphate (AMP) (64). As a result of mTORC1 inactivation and AMPK activation, the ULK1 kinase loses its repressive phosphorylation on S757 and gains an activating phosphorylation at S555 (65). Activated ULK1, in complex with ATG13 and FIP200, together with the PI3K complex, consisting of VPS34, VPS15, BECLIN-1 and ATG14L recruit autophagy proteins to the site of autophagosome biogenesis. The PI3K complex is responsible for increasing the pool of PI3P at the sites of autophagy initiation and is required for recruitment of downstream autophagy proteins (66). Autophagy proteins are recruited to the autophagy start sites by binding PI3P via PI3P interacting regions such as FYVE domains (67) or WD40 repeats (68). Autophagy is controlled by mTORC1. However, this process can be self-regulating, since amino acids released from lysosomes after autophagic degradation through trans-membrane amino acid transporters activate amino acid sensors localized at the lysosomal membranes, CASTOR1 (69) and SLC38A9 (70). The increase in amino acids close to the lysosomal surface recruits and activates mTORC1 at the lysosome (71), thereby forming a negative feedback loop to inhibit autophagy.

ER stress is also a known regulator of autophagy. The unfolded protein response (UPR) is a response towards increased unfolded and misfolded protein in the ER lumen to restore normal ER function. For example, the autophagic process assists ER stress recovery by removing excessive ER membrane after stress induction by targeting ER membrane compartments to the autophagosomes through the LIR of SEC62 of the ER translocon complex (72). The UPR and autophagy are two interconnected homeostatic systems, whereby branches of the UPR are able to induce autophagy and vice versa. ER stress induces the phosphorylation of the stress regulated protein kinase c-Jun N-terminal kinase 1 (JNK1) which in turn phosphorylates B-cell lymphoma 2 (BCL2), thereby relieving Beclin 1 (BECN1) from its inhibition by BCL2 and allowing autophagic progression (73). Activation of the UPR induces splicing of *XBP1*, which translocates into the nucleus to upregulate BECN1 expression and drive autophagy (74). The eiF2α/ATF4 branch of the UPR sustains transcriptional upregulation of autophagy genes during amino acid starvation (75), promotes cell survival through upregulation of ULK1 (76) and is required for autophagy upregulation and treatment resistance after treatment with the proteasome inhibitor bortezomib (77).

Inflammation regulates and is itself regulated by autophagy. Optineurin, an adaptor protein indispensable for mitophagy (31), has been shown to compete with NF-kappa-B essential modulator (NEMO) for binding to polyubiquitinated Receptor-interacting protein (RIP) via its ubiquitin binding domain, functioning therefore as a competitive inhibitor of the TNFα signaling pathway (78). p62 has also been shown to interact with TRAF6, an E3 ubiquitin ligase, resulting in polyubiquitination of TRAF6 and NF-kB activation (79) while Paget's disease of bone (PDB) mutations in p62 increase NF-kB pathway activation (80). Furthermore, p62 is necessary for TRAIL induced apoptotic signaling through its association to and recruitment of caspase 8 to characteristic p62-enriched structures referred to as speckles (81). Autophagy is indispensable for the production of IFNα by dendritic cells by delivering viral nucleic acids to Toll-like Receptors (TLRs) located in endosomes (82).

Transcription factors (TFs) regulate the abundance of autophagy proteins at the transcriptional level to regulate its flux. ATF4 (75), PPARα (83), NF-κB (84), CREB (85) and TFEB (86) are examples of TFs that are able to bind to regulatory regions of autophagy genes to regulate their expression. TFEB overexpression is sufficient to induce autophagy whereas depletion of TFEB decreases lysosomal size and number and the autophagic flux (86). TFEB is found in both the cytosol and the nucleus, and its function is dependent on nuclear translocation. This translocation is regulated by its interactions to the scaffold protein 14-3-3 which, when bound,

sequesters TFEB in the cytosol. This interaction to 14-3-3 is dependent on the phosphorylation on TFEB on S142 and S211, which has been shown to be a direct substrate of the Ser/Thr kinase complex mTORC1 (87, 88). This repressive binding to TFEB can be reversed by dephosphorylation mediated by the calcium driven phosphatase, calcineurin (89). Calcium released from the lysosomes, through the lysosomal ion channel MCOLN1, activates Calcineurin, which in turn removes the phosphorylation on TFEB, alleviating it from 14-3-3 inhibition. The nuclear localization signal of TFEB is now exposed and the transcription factor is able to translocate into the nucleus to drive lysosome gene expression (89).

## 1.2.4 Autophagy and cancer

Autophagy has been described as a double edged sword, playing roles in both promoting and suppressing cancer (90). On one side, autophagy prevents cancer initiation during the initial phases of carcinogenesis; by turning over damaged organelles such as mitochondria, lysosomes and ER, the cell is able to reduce the buildup of damaging reactive oxygen species (ROS) and cellular waste that may promote DNA damage and downstream proliferative signaling. On the other side, towards the later stages of oncogenesis, autophagy is protective towards the microenvironmental stress faced by a rapidly growing tumor to survive and proliferate.

Cellular byproducts such as ROS are reactive molecules formed from the reduction of oxygen and are found in abundance in tumors where they may promote tumor development (91). However, ROS also function as signaling molecules to induce cell signaling events, such as the cyto-protective antioxidant-signaling pathway Nrf2-Keap1 (92). Recent findings have described the intersection between the antioxidant-signaling pathway and autophagy. The autophagic adaptor protein p62 targets Keap1 to the autophagosome for its destruction, thereby stabilizing the transcription factor Nrf2 and leading to prolonged target gene expression (93) while overexpression of p62 in mice xenograft models results in increased tumor burden (94). The loss of p62 on the other hand leads to enhanced cellular ROS, which is the result of reduced NF-κB activation and subsequent expression of ROS scavengers (94, 95). ROS may therefore form a possible negative feedback loop where p62 leads to decreased ROS generation that prevents damage from free radicals but also leads to prolonged activation of signaling pathways.

Growing tumors are often faced with multiple challenges as they increase in size. As they grow, cells closer to the core of the tumor are often hypoxic due to decreased accessibility to the vasculature and blood circulation. This increase in demand for oxygen, nutrient and waste

circulation is overcome by angiogenesis, which is the formation of new blood vessels partly through activation of hypoxic signaling through Hypoxia-inducible factor alpha (HIF1α). In addition to angiogenesis signaling, HIF1α also induces autophagy by transcriptionally upregulating BCL2 interacting protein 3 (BNIP3) that relieves the repression of BCL-2 on BECN1 (96). Hypoxia signaling is itself regulated by autophagy, where HIF1α is degraded in the lysosomes by CMA (97). In addition to HIF1α, hypoxia induced autophagy is also instigated by PKCδ through JNK1 but not JNK2 (98). Presumably, due to the lack of oxygen to function as electron acceptors, FUN14 Domain containing 1 (FUNDC1) driven mitophagy is upregulated during hypoxic conditions in HeLa cells (99). This allows for quality control of dysregulated mitochondria.

Metastasis is the process whereby cancer cells from a primary tumor are able to escape into the circulation and colonize distant organs. The metastatic cascade is made up of several stages: local invasion, intra-vesation into the circulatory system, migration, extravasation and eventually colonization. Autophagy enables migrating cancer cells to establish themselves in new, unfamiliar and foreign microenvironments. True to this concept, LC3 punctate structures were found to be higher in breast cancer (BCa) and melanoma metastasis (100, 101). Anoikis, a form of cell death driven by loss of attachment to the extra-cellular matrix is repressed by autophagy (102). The SRC kinase is targeted by Casitas B-lineage Lymphoma (c-Cbl) for degradation by autophagy, thereby promoting cell survival when focal adhesion kinase (FAK) activity is low during cell migration (103). Autophagy also plays a role in both inhibiting and promoting metastasis. Focal adhesion kinase family integrating protein (FIP200), a member of the ULK1 kinase complex, represses the autophosphorylation of the FAK which inhibits cellular migration (104).

Cancer cells have increased survival, driven partly by a repressed or aberrant apoptotic signaling. BCL2 is capable of binding to either pro-apoptotic Bcl-2-associated X protein (BAX) and Bcl-2 homologous antagonist killer (BAK) or BECN1 (105). This binding of BCL2 sequesters either BAX/BAK or BECN1, allowing the formation of either the apoptotic or autophagic complex at any given time. BCl2-binding is therefore a switch whereby either apoptosis or autophagy dominate.

## 1.2.5 Autophagy and cancer treatment

Autophagy is a mechanism that aids cell survival in the face of micro-environmental stress, and is thus beneficial for cancer cell survival during treatment. The widely used chemotherapeutics paclitaxel and docetaxel inhibit microtubule function and prevent autophagosome-lysosome fusion, effectively blocking autophagy (106). Ionizing radiation during radiotherapy induces autophagy through decreasing the amount of activating, phosphorylated mTOR (107) and activating the UPR by inducing protein kinase R-like endoplasmic reticulum kinase (PERK) expression (108), both of which are events that were previously reported to induce autophagy (109).

Tamoxifen is the mainstay treatment of estrogen receptor (E2R) positive BCa. This prodrug is taken up orally and is processed in the liver into 4-hydroxytamoxifen (4-OHT), which has significantly stronger affinity to the E2R and therefore outcompetes estrogen for binding to the active site in the E2R. As for many other chemotherapeutics, there have been multiple observations where autophagy is activated upon tamoxifen treatment and that a functional autophagic machinery is a prerequisite for tamoxifen resistance (110-113).

Other treatments, although not specifically targeting the autophagic pathway, affect autophagy consequentially. BH3 mimetics such as ABT-737 (114) sequester and inhibit pro-survival Bcl-2 family proteins, leading to mitochondrial cytochrome c release. Bcl-2, interestingly regulates the balance between apoptosis and autophagy by binding to BECN1 complex to inhibit its activity, and Bcl-2 homology (BH3) mimetics relieves BECN1 from its repression by Bcl-2 leading to activation of autophagy (115, 116).

The findings described above have generated interest in the manipulation of autophagy during cancer treatment. There are currently >50 clinical trials listed on clinicaltrials.gov where autophagy is being targeted in cancer patients. Many of these clinical trials harness the well-documented pharmacodynamics and pharmacokinetics of hydroxychloroquine and chloroquine, inexpensive and accessible lysothropic drugs currently used in the treatment of patients diagnosed with malaria or rheumatoid arthritis (117). Hydroxychloroquine and chloroquine are lysosomotrophic bases that accumulate in the lysosomes leading to neutralization of $H^+$. The pH increase in the lysosomal lumen are inhibitory to resident lysosomal cathepsins and proteases, which prevents lysosomal degradation and thus resulting in autophagy inhibition. Interestingly, treatment with chloroquine inhibits the activation of

mTORC1, which relieves the repressive phosphorylation on TFEB and ULK1 (118). As such, chloroquine is capable of both activating and preventing autophagy.

## 1.2.6 Autophagy and prostate cancer

Early staged PCa is often treated through a regiment of different therapeutic options including surgery, radiation therapy, cytotherapy, chemotherapy and ADT. ADT in PCa is often initially effective. Regrettably, the tumors eventually advance to ADT-insensitive, castration-resistant PCa that is no longer dependent on androgens but is still positive for AR signaling (21). Although an array of reports indicated that activation or disruption of AR signaling could affect autophagy levels in PCa cells, the observations have been mixed.

Kaini et al. showed that androgen depletion induced autophagy and lipid droplet degradation through lipophagy (119), while siRNA mediated AR knockdown induced autophagy and reintroduction of functional AR decreased autophagic flux (120). Similarly, supplementation of dihydrotestosterone (DHT) decreased autophagy in LNCaP through mTOR activation (121). AR inhibition by ADT using non-steroidal AR antagonists such as bicalutamide induces autophagy in PCa cells in the presence and absence of external cellular stressors (122). Furthermore, interference of AR function using enzalutamide induces increased autophagy in *in vitro* and *in vivo* models (123). This induction of autophagy upon ADT appears to be protective as Benett et al. showed that the androgen insensitive LNCaP-AI cells were roughly twice as resistant to docetaxel than to the androgen sensitive LNCaP, and re-supplementation of LNCaP-AI with androgens decreased docetaxel sensitivity (123). Inhibition of autophagy and suppression of androgen signaling were combinatorially repressive on PCa cell growth (124), a finding that has led to multiple clinical trials involving ADT and androgen receptor inhibition in PCa. However, androgen regulated autophagy cannot completely be attributed to AR function as autophagy is also induced in PC3 cell lines which do not express AR during ADT (121).

In contrast, Shi et al. found that the synthetic androgen R1881 increased the autophagic flux after 3 days in LNCaP and VCaP cells and induced intracellular lipid accumulation (125). The same group further show that the AR activates autophagy by directly regulating the expression of the transcription factor TFEB and four core autophagy genes, ATG4B, ATG4D, ULK1 and ULK2 (126). A unifying explanation is therefore required to explain the mechanisms behind

the relationship between androgen signaling and autophagy activation in PCa such that this knowledge can be effectively translated to the bedside.

TNFα-dependent apoptotic cell death is enhanced upon androgen induction by rapamycin treatment in the AR negative PCa cell line PC3, while it is potentiated by the PI3K inhibitor 3-Methyladenine in LNCaP cells (127). Metformin, an AMPK activator commonly used to treat diabetes type II, has been shown to repress proliferation in multiple cancer cells lines, PCa included. Metformin activates AMPK in PCa, leading to inhibition of mTOR, which would set metformin as an autophagy inducer but confusingly it represses autophagy, through mechanisms that are yet to be fully determined (123). This finding is further supported by data which show that diabetic patients taking metformin have lower incidence of PCa (128). A combination of enzalutamide and metformin significantly decreased xenograft tumor sizes while LNCaP and PC3 cells treated with bicalutamide and metformin decreased cancer cell colony formation (129).

Nonetheless, targeting specific components of the autophagic machinery during cancer therapy is complicated due to the heterogeneity of PCa tumors. This is reflected in the stark differences in the status of autophagy in PCa derived cancer cell lines. For example, DU-145, a cell line derived from metastasis in the central nervous system lacks expression of canonical ATG5 transcripts and has very little to no lipidated forms of LC3, as compared to other PCa cell lines, LNCaP and PC-3 (130).

# 1.3  Six Transmembrane protein of the prostate (STAMP)
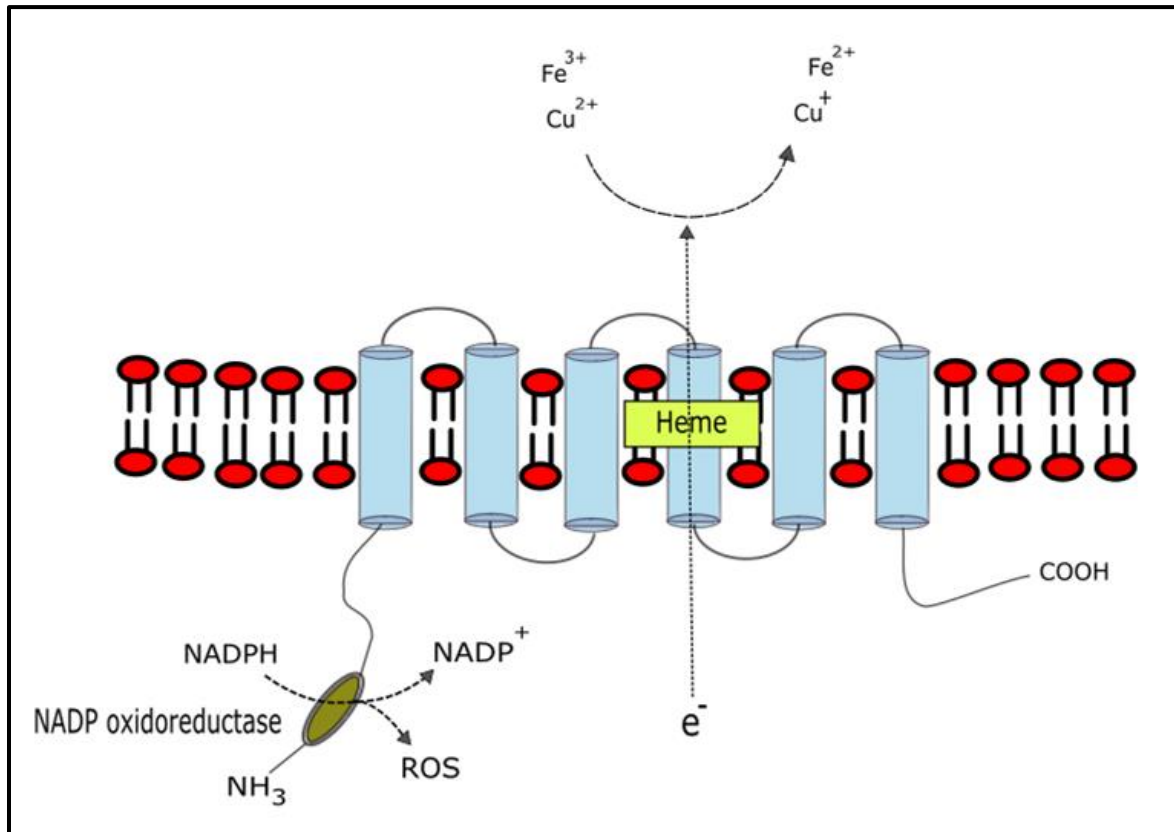
## 1.3.1 The STAMP family



**Figure 3. The structure of the STAMP family proteins.** The STAMP family proteins contain a dinucleotide binding motif that is necessary for the recruitment of FAD and a NADP oxidoreductase domain that oxidizes NADPH. STAMPS catalyze the reduction of $Fe^{3+}$ and $Cu^{2+}$ to $Fe^{2+}$ and $Cu^+$ respectively.

STAMPs are a family of transmembrane proteins that traverse biological lipid membranes through six hydrophobic transmembrane domains (131, 132). The transmembrane domains are flanked by a long amino terminus and short carboxyl terminus, both of which are predicted to face the cytosol. The STAMP family is comprised of STAMP1, STAMP2 and STAMP3, each sharing significant sequence similarity to the F(420)H(2):NADP(+) oxidoreductase present in archaea and bacteria at the disordered N-terminal (133). Furthermore, the STAMPs share notable homology in their COOH-terminal domain to the transmembrane protein of the FRE metalloreductases in yeast (134). Consistent with this the STAMPs were shown to possess ferri- and cupricreductase activity (135). Ferri- and cupricreductases reduce ferric iron ($Fe^{3+}$) to ferrous iron ($Fe^{2+}$), and cupric copper ($Cu^{2+}$) to cuprous copper ($Cu^+$), which are necessary for

their transport from endosomal compartments into the cytosol through the divalent metal transporter (DMT1) (136). The proposed model for the catalytic activity of the STAMP family proteins are as follows: NADPH plays the role of the initial electron donor and is oxidized by the NADP oxidoreductase domain. These electrons are then delivered subsequently to the FAD and heme groups located within the transmembrane region. The electrons, through the ferrireductase domain, reduce ferric iron to ferrous iron. STAMPs are predicted to bind to iron and copper through conserved histidine residues that are responsible for binding to heme groups (137, 138). Corroborating the proposed role of STAMPs in cellular metal transport, STAMP2 has been shown to regulate cellular iron levels in osteoclasts during osteoclastogenesis (139), and STAMP3 knockdown induced an anemia-like phenotype in macrophages and hepatocytes (136). However, the functions are not limited to metal transport and as described below, the STAMPs, although sharing structural and sequence similarities, appear to have both different and redundant functions in various aspects of cellular biology.

All members of the STAMP family localize to early endosomal structures indicating that they may be involved in endocytic/endosomal recycling pathways (134, 140, 141) .The STAMPs share a common YXXØ consensus sequence that is consistent with their localization to endosomes (142). The cellular localization of the STAMPs is summarized in Table 1.

| | Localization | Colocalization | Cell/Tissue type | Reference |
|---|---|---|---|---|
| **STAMP1** | Early endocytic vesicles, Golgi apparatus, Plasma membrane | TfR, EEA1 | LNCaP and CWR22 (Prostate) | Korkmaz et al., 2002; Porkka et al., 2002 |
| **STAMP2** | Early endocytic vesicles, Golgi apparatus, ER, Plasma membrane | TfR, EEA1, FAK, Caveolin-1 | LNCaP (Prostate) 3T3-L1 (Adipose) Human oemental adipose tissue | Korkmaz et al., 2005; Yang et al., 2001; Chambaut-Guerin et al., 2005; Zhang et al. 2008 |
| **STAMP3** | Early endosomes, Exosomes | TfR, DMT1, TCTP | HEK293T (Embryonic kidney) | Ohgami et al., 2005b; Amzallag et al., 2004 |

**Table 1. Summary of STAMP cellular localization.**

Expression of GFP-tagged STAMP1 indicates that the transmembrane protein traffics between the Golgi apparatus and the plasma membrane. TNFα-induced adipose related protein (TIARP), the mouse homologue of STAMP2, was also present at the plasma membrane in adipocytes (88).

## 1.3.2 STAMP expression

STAMP1 is highly expressed in the prostate and to a significantly lesser extent in several other tissues (135, 140, 143). STAMP1 is not expressed in AR-negative PCa cell lines such as PC3 and DU-145 and thus appear to be dependent on AR for its expression. Interestingly, STAMP1 transcription is not androgen-regulated despite the requirement of functional AR in the cell for its expression. STAMP1 expression correlated positively with disease severity in PCa (140, 143, 144). In murine preadipocytes, *STAMP1* is decreased during adipogenesis (145). Inflammatory signaling has also been shown to affect STAMP1 mRNA transcription as activation of the NF-κB pathway following TNFα treatment decreased STAMP1 expression (146).

STAMP2 mRNA is found in multiple organs, with the highest expression in the bone marrow, lung, white and brown adipose tissues, prostate, liver, heart, skeletal muscles, small intestines and kidney (135, 141, 147, 148). The regulation of STAMP2 expression has been studied in greater depth compared to STAMP1. Similar to STAMP1, STAMP2 expression increases with PCa progression (141, 149); however, unlike STAMP1, STAMP2 is upregulated upon differentiation in pre-adipocytes in 3T3-L1 and hASC mouse and human pre-adipocytes (145, 148, 150) and by androgens (141, 149). In addition to adipocyte differentiation, *STAMP2* increases during the biogenesis of osteoclasts and is required for regulation of cellular iron uptake (139). However, the most striking regulator of STAMP2 expression in the cell is possibly nutrient availability and metabolic signaling. Feeding of hepatic and adipocyte cells induces the transcription of *STAMP2*, while its expression is greatly decreased upon fasting (148, 151). Notably, *STAMP2* in subcutaneous and visceral white adipose tissues (VWAT) is increased in obese mice models (147) while it is decreased in livers of non-alcoholic fatty liver disease (NAFLD) human patients and in NAFLD mice under a high fat diet (152), indicating an important role of STAMP2 in the development of obesity. The STAMP2 homologue in mice was first described as TIARP, a plasma membrane transmembrane protein that is induced by TNFα (153). Similar to its homologue, *STAMP2* is also positively regulated by multiple

cytokines such as TNFα (148, 154, 155), IL-6 (151, 156), IL-Iβ (157), IL-17 (158) and Lipopolysaccharides (LPS) (159, 160).

In parallel to *STAMP2*, *Stamp3* is also increased in differentiating 3T3-L1 murine preadipocytes (145). Iron is an important molecule in multiple enzymes, playing important roles as cofactors necessary for biochemical reactions in the active site. Hypoferric conditions induce the expression of STAMP3 (161), possibly reflecting a cellular compensatory mechanism to increase cellular iron uptake. Eliciting the immune response with LPS however decreases STAMP3 expression (136).

The control of STAMP expression in response to various signaling molecules and cellular processes suggests that the STAMPs are themselves more than just bystanders but are directly involved in the regulation of the respective signaling pathways involved.

## 1.3.3 Physiological and cellular functions of the STAMPs

The STAMPs contain a C-terminal ferrireductase domain that is necessary for iron translocation into the cytoplasm during transferrin-dependent iron uptake. Mutations in STAMP3 decreased the amount of ferric reductase activity in the blood and higher concentrations of iron and copper in the liver in C57BKL/6 mice (162). In primary hippocampal neurons, STAMP1 was also found to colocalize to components of the transferrin-dependent iron cycling (135) and was suggested to be involved in translocation of iron through the blood brain barrier (163). STAMP2 depletion in osteoclasts greatly decreased the levels of intracellular soluble iron (139), indicating its importance in iron uptake.

In contrast to the role of STAMP1 as a proliferative factor in PCa (140), STAMP3 appears to play the opposite role as a tumor suppressor. pHyde, the homologue of STAMP3 in rats induces apoptosis in PCa cells when ectopically expressed, while viral transduction of STAMP3 in human PCa cells inhibited cell growth and promoted apoptosis (164). STAMP3 expression is regulated by the tumor suppressor protein p53 and through direct interactions with Nix and Myt1 is able to drive apoptosis and repress cell cycle progression (165). The localization of STAMP3 to endocytic compartments and its regulation by p53 during DNA damage is relevant for its role as the moderator in p53 mediated exosome secretion (166). External factors also influence STAMP3 expression as smoking induces STAMP3 expression by two fold in Crohn's

disease patients, a chronic inflammatory bowel disease (167), suggesting that STAMP3 may be involved in colon function and biology.

As its complex regulation would suggest, STAMP2 is involved in multiple aspects of cellular biology. Most investigations into the role of STAMP2 in cells has been performed in the context of metabolic syndrome and obesity. In *in vivo* mice models, feeding induces the expression of STAMP2 in VWAT. This response to feeding is greatly reduced in obese mice. siRNA mediated knockdown of STAMP2 in murine 3TL3-L1 adipocytes led to decreases in both insulin sensitivity and glucose uptake, while both macrophage recruitment and inflammatory gene expression was increased (148). Considering this, STAMP2 protein and mRNA levels in adipose tissues were upregulated in obese patients from Sweden (147). Consistent with this result STAMP2 mRNA is increased in VWAT and brown adipose tissues (BAT) in obese mice. In hepatocytes, STAMP2 attenuates high fat diet induced insulin resistance whereby ectopic expression of STAMP2 improves insulin resistance in high fat diet treated mice (152). Further corroborating the importance of STAMP2 for metabolic homeostasis, insulin action is decreased in STAMP2 deficient mice and induction of STAMP2 after feeding is greatly decreased in obese mice (148, 159). The effect of STAMP2 loss on insulin induced glucose uptake can be explained by the decrease of glucose transporter 4 (GLUT4) translocation to the plasma membrane thereby preventing glucose transport in part by attenuating protein kinase B (AKT) phosphorylation (168).

In STAMP2 knockout macrophages treated with LPS, interleukin-16 (IL-6) and inducible nitric oxide (iNOS) expression was increased, suggesting that STAMP2 may repress inflammatory signaling. This is true in both human and mice microphages, where STAMP2 represses inflammation and protects against atherosclerosis through modulation of NADPH levels, in part through degradation of p65 by nuclear translocation of the NADPH sensor NmrA-like family domain-containing protein 1 (NMRAL1) and activation of copper metabolism domain containing 1 (COMMD1) (159). Adipocyte and osteoclast differentiation is dependent on STAMP2 as osteoclast formation is inhibited by STAMP2 knockdown (139), and adipocyte differentiation of 3T3-L1 is significantly reduced upon STAMP2 depletion (145). STAMP2 may therefore play a role in cellular differentiation in addition to protecting the cell against excessive nutrient surplus and aberrant inflammatory signaling.

Ectopic expression of STAMP2 in the human embryonic kidney 293T cells grown in suspension hinders anchorage independent cell growth possibly through the activation of FAK

(169). In addition to the decrease in cell growth, the activating phosphorylation of FAK1 on tyrosine-397 was also shown to be decreased while the inhibition on cell growth could be rescued by supplementation of antibodies against STAMP2 in the culture media. The effects of STAMP2 overexpression on anchorage-free cell survival was attributed to the possible direct interactions between STAMP2 and FAK as shown by immunoprecipitation (169). This suggests that STAMP2 could be involved in facilitating cellular attachment and motility (168).

## 1.3.4 STAMP2 in prostate cancer

As described earlier, STAMP2 expression is tightly regulated by androgens (141). As such, STAMP2 protein is decreased when androgens are depleted during ADT, but is greatly increased upon the formation of CRPC. Histological and *in silico* analysis of PCa specimens show that STAMP2 expression is increased in advanced and metastasized PCa (141, 149), suggesting a role of STAMP2 as a potential oncogene in PCa. siRNA mediated knockdown of STAMP2 inhibited tumor colony formation and PCa cell growth, while overexpression of STAMP2 rescued these cells from this inhibition and promoted prostate cell proliferation. shRNA mediated STAMP2 knockdown in *in vivo* tumors subcutaneously implanted into male SCID mice greatly reduced tumor growth. Furthermore, loss of STAMP2 led to increased fraction of cells in the G0/G1 phase, indicating partial cell cycle arrest (149). This was shown to be dependent on its ferri-reductase activity, increases in intracellular reactive oxidative species (ROS) and activation of the stress transcription factor ATF4. Interestingly, despite its AR negative status, shRNA knockdown of STAMP2 in androgen-insensitive 22Rv1 cells also decreased PCa cell and tumor growth (149). The knockdown of STAMP2 in adipose stem cell-derived adipocytes prevented PCa tumor growth in nude mice, possibly caused by decreases in adipokine secretion (170). This shows that STAMP2 levels in the supporting stroma also play a role in determining PCa tumor growth. The observations described so far suggest that STAMP2 may function as a molecular target and as a biomarker in the detection of PCa.

# 2   Aims of Study

The major aim of this study is to further our understanding of the complex regulation of autophagy in PCa, with a focus on the role of STAMP2 whose expression is androgen regulated. Efforts to target autophagy in conjunction with androgen inhibition and chemotherapeutic drugs in PCa are promising in *in vitro* and *in vivo* settings although it has yet to yield improved therapeutic outcome in clinical trials. This delay could be largely explained by the lack of understanding the complex mechanisms of autophagy in PCa. Previous studies carried out in our laboratory have shown that STAMP2 may influence transcription factors involved in maintaining gene expression during starvation-induced autophagy. Our initial hypothesis was that STAMP2 may potentially promote autophagy by upregulation of autophagy genes, thereby providing a survival advantage to cells with increased levels of oncogenic STAMP2. In addition to ROS, STAMP2 also affects multiple signaling pathways such as inflammation and insulin signaling in PCa, which in turn are known autophagy regulators. We thus set out to elucidate in detail the potential involvement of STAMP2 in autophagy in PCa. This thesis describes our efforts to test the aforementioned proposed hypothesis.

# 3   Materials and methods

## 3.1  Materials

| AppliChem, Darmstadt, Germany. | Roche Diagnostics Corp., IN, USA. |
|---|---|
| - Polyacrylamide (40%) | - Lightcycler 480 SYBR green I Master |
| | - Magnesium Chloride (MgCl$_2$) |
| **BI Biological Industries, Kibbutz BeitHaemek, Israel.** | - 4-(2-Hydroxyethyl)piperazine-1-ethanesulfonic acid (HEPES) |
| - Fetal bovine serum (FBS) | - Acetic acid |
| | - Ammonium persulfate (APS) |
| **BioRad Laboratories Inc., Hercules, CA, USA.** | - Bovine serum albumin (BSA) |
| - Clarity$^{TM}$ Western ECKL substrate cat.# 170-5060 | - Bromophenol blue |
| | - Chloroform |
| - Immunoblot$^{TM}$ polyvinylidene fluoride (PDVF) membrane | - Non-fat dry skimmed milk |
| | - Ethidium bromide (EtBr) |
| | - Glycine |
| **BD Biosciences** | - Horseradish peroxidase (HRP)-conjugated a-mouse IgG antibody |
| - p62 mouse pAb | |
| - Precision Plus Dual Color protein standard | - Horseradish peroxidase (HRP)-conjugated a-rabbit IgG antibody |
| | - Phenylmethylsulfonyl fluoride (PMSF) |
| **Biotool, Selleck Chemicals** | - PhosStop phosphatase inhibitor |
| - All-in-one cDNA Synthesis SuperMix, cat.#B24408 | - Protease inhibitor cocktail (PIC) |
| | - Sodium azide (NaN$_3$) |
| **BioWhittaker-Lonza, Rockland, ME, USA** | - Sodium dodesyl sulphate (SDS) |
| - DMEM 1640 media, cat.#BE12-709F | - Tetramethylethylenediamine (TEMED) |
| - L-glutamine cat.#BE17-605E | - Octyl phenoxy polyoxy ethanol (Triton X-100) |
| - MycoAlert Mycoplasma Detection Kit | - Whatman cellulose chromatography papers |
| - Penicillin/Streptomycin, cat.#DE17-603E | |
| - RPMI 1640 media, cat.#BE12-115 | **Kimetyl AS, Halden, Norway** |
| - SeaPlaque Agarose | - Ethanol 100% |
| - Trypsin EDTA, cat.#CC-5012 | |

**Cell Signaling**
- ULK1 rabbit pAb ca.# 4776
- P-ULK1 (S757) rabbit pAb ca.#6888S
- P-ULK1 (S555) rabbit pAb ca.#5869S
- TFEB rabbit mAb ca.#4240S

**Enzo Life Sciences**
- Bafilomycin A1 inhibitor, cat.#BML-CM110-0100

**Proteintech, Manchester, U.K.**
- HDAC1 rabbit pAb
- STAMP2 rabbit pAb

**QIAGEN**
- siRNA

**Santa Cruz Biotechnology Inc., Santa Cruz, CA, USA.**
- GAPDH mouse mAb

**ThermoScientific**
- Subcellular protein fractionation kit for cultured cells, cat.# PI78840

**MBL**
- LC3 rabbit pAB, cat.#PM036

**Sigma-Aldrich, St. Louis, MO, USA.**
- 10x PBS
- Isopropanol
- 37% HCL
- Dimethyl sulfoxide (DMSO)
- Oligo-dT reverse transcription primer
- PCR primers
- R1881 (synthetic androgen)
- TRI-reagent, cat.#T9424
- Trichloroacetic acid (TCA)
- Tween-20'
- B-Actin pAb

**Invitrogen, Carlsbad, CA, USA.**
- Dithiothreitol (DTT)
- Superscript$^{TM}$ II Reverse Transcriptase kit, cat.#18064

**Life technologies, Thermo Fisher Scientific Inc.**
- Lipofectamine RNAiMAX
- Lipofectamine 3000
- Goat anti-Rabbit IgG Secondary Antibody, Alexa Fluor 488

**New England biolabs Inc., Ipswich, MA, USA.**
- 2-Log DNA ladder
- DNA loading ladder
- dNTP (deoxyribonucleotide)

**Open Biosystems, Thermo Scientific**
- STAMP2 shRNA

**Perkin Elmer**
- Valine, L-[U-$^{14}$C], cat.# NEC291EU050UC
- UltimaGold Liquid scintillation cocktail ca.# 6013329

**Promega, Madison, WI, USA.**
- Recombinant RNasin Ribonuclease Inhibitor

**Qiagen**
- STAMP2 siRNA

**VWR International, Leuven, Germany.**
- Ethylenediaminetetra-acetic acid disodium salt (EDTA)
- Methanol
- Sodium chloride (NaCl)
- Sodium hydroxide (NaOH) Tris(hydroxymethyl)aminomethane

## 3.2  Methods

**Cell culture**

Human prostate cancer cell line LNCaP was acquired from the American Type Culture collection (ATCC# CRL-1740) and maintained in RPMI 1640 (Lonza). Vertebral metastasis derived prostate cancer cell line VCaP (ATCC#CRL-2876) was maintained in Dublecco's Modified Eagle's Medium (DMEM, Lonza). The cells were cultured in a sterile humidified 5% $CO_2$ incubator at 37°C in their respective growth media containing 10% Fetal Bovine Serum (FBS), 5 mg/ml penicillin/streptomycin, and 4 mM $L$-Glutamine, and maintained at a passage below 30. The culture medium was changed every 2-3 days. All cells were confirmed to be mycoplasma free using the MycoAlert Mycoplasma Detection Kit (Lonza). Synthetic androgen R1881 (Sigma) was dissolved in 96% ethanol and was kept shielded from light at -20°C. Where stated, R1881 was added to the tissue culture media to obtain a final concentration of 1 nM. For starvation treatments, cells were washed in PBS and cultured in EBSS (GIBCO) for the indicated times. Bafilomycin (Enzo) was reconstituted in DMSO and kept at -20°C. Bafilomycin was added to the media to obtain a final concentration of 100nM for no longer than 4 hours. Lysosomes were stained by incubating cells in prewarmed medium containing 75nM Lysotracker Deep Red (Life technologies) for 30 minutes at 37°C.

**RNA interference**

Gene knockdown was performed using Lipofectamine RNAiMax (Invitrogen) according to manufacturer's protocol for reverse transfection. The siRNA-Lipofectamine transfection was first prepared and added into empty tissue culture dishes/plates. Trypsinized cells resuspended in RPMI 1640 medium (10%FBS) were then added to the transfection mixture to obtain a final siRNA concentration of 10nM. The siRNA oligonucleotide used was STAMP2-In3 (Qiagen) AATGCAGAGTACCTTGCTCAT.

**SDS-PAGE**

Prior to harvesting, the cells were washed twice with ice cold PBS. The cells were scraped and pelleted by centrifugation at 4 degrees by centrifugation at 3000 rpm for 5 minutes. The cells were incubated in 2 times the volume of the pellet of RIPA lysis buffer (150 mM NaCl, 5 mM EDTA, 50 mM Tris, 1% NP-40, 0.5% Sodium deoxycholate, 0.1% SDS) for 1 hour. To remove cell debris, the lysed cells underwent centrifugation at 13,000 rpm for 15 minutes and the

supernatant (whole cell extract) was collected. Protein concentrations were determined using the Bradford Protein assay with BSA standard curve reference according to manufacturers instructions. Equal amounts of protein extract (30-40µg) were mixed with SDS sample buffer (200 mM Tris-HCl (pH 6.8), 400 mM DTT, 8% SDS, 0.4% bromophenol blue, 40% glycerol) and heated at 95°C for 5 minutes. The protein samples were separated 12% SDS-page gels (Stacking gel : 5% polyacrylamide, 125 mM Tris-HCl pH 6.8, 0.04% APS, 0.1% SDS and 0.1% TEMED; Seperating gel : 12% polyacrylamide, 375 mM Tris-HCl pH 8.8, 0.04% APS, 0.1% SDS and 0.1% TEMED) at 90-120 V in SDS running buffer (25 mM Tris-HCl, 192 mM glycine and 0.1% SDS). Precision Plus Protein dual protein standard (Bio-Rad) was used to estimate the protein sizes of each band. After electrophoresis, the proteins were transferred to methanol activated PVDF membrane (Bio-Rad) in semi dry transfer buffer (50 mM Tris, 40 mM glycine and 1.2 mM SDS) containing 20% methanol.

**Western blot analysis**

After semi-dry transfer, membranes were then blocked in 5% non-fat milk diluted in tris-buffered saline with tween (TBS-T, 0.2M Tris, 1.4M NaCl, 0.1% Tween-20) for 1 hour, followed by overnight incubation in primary antibody dissolved in TBST containing 5% BSA and 0.05% $NAN_3$. The membranes were then incubated in secondary antibodies (HRP-conjugated anti-rabbit IgG antibody (1:10000 dilution) or HRP-conjugated anti-mouse IgG antibody (1:10000 dilution)) in TBST for 1 hour at room temperature. Primary antibody dilutions were α-ACTB (1:2000), α-LC3 (1:1000), α-p62 (1:1000), α-P-ULK1 (S555/S757, 1:1000), α-P-p70S6K (1:1000), α-P-AMPK (1:1000), α-p70S6K (1:1000), α-AMPK (1:1000), α-TFEB (1:1000), α-HDAC1 (1:1000) and α-GAPDH (1:1000). Chemiluminescence was detected using the Clarity HRP substrate (BioRad) and detected using a Kodak 4000R Image Station. Stripping for reprobing was carried out by incubating the membrane in mild stripping buffer (200 mM glycine, pH 2.5, 2% SDS) on a rocker for 3 x 15 minutes followed by 3 x 5 minutes washing in PBS.

**Synthesis of cDNA and RT-qPCR**

RNA was extracted by incubation in TRIzol Reagent as described by the manufacturer's instructions. RNA pellets were washed twice in 70% EtOH and resolved in DEPC-treated H2O. The RNA purity and concentration were determined using NanoDrop 1000 (ThermoScientific, Nanodrop technology). RNA integrity was assessed by agarose gel electrophoresis. 0.5µg total

RNA was added to Nucleotides, Oligo-dT, First Strand Buffer, 0.1 M DTT, RNase inhibitor, DEPC H$_2$O and SuperScript II Reverse Transcriptase. The mixture was used to synthesize cDNA by incubating at 42$^o$C for 1 hour, and the reaction was inactivated at 70$^o$C for 5 minutes.

Analysis of real time PCRs were performed using the Light Cycler (Roche) in 96-well plates with 10µl total reaction volume, containing 1X Lightcycler 480 SYBR Green 1 Master mix, 0.5 µM forward primer, 0.5 µM reverse primer. The cDNA was diluted 1:10 in nuclease free water. 4 µl of the diluted cDNA solution was mixed with 0.5µl of both reverse and forward primers (10 µM) and 6 µl of SYBR Master Mixture. The mixture was then added to qPCR plates. The qPCR was run at 45 cycles of denaturing at 95$^o$C for 10 sec, annealing at 60$^o$C for 10 seconds, and elongation and fluorescence reading at 72$^o$C for 20 seconds. Crossing Point (Cq) values were used to calculate mRNA concentrations. Cq values of the genes were normalized to the housekeeping gene TBP. Results were presented in the form of relative gene expression.

**Primers**

| Target | Forward primer | Reverse primer |
|--------|----------------|----------------|
| *MAP1LC3B* | CAGCTTCCTGTTCTGGATAAA | GCTGTAAGCGCCTTCTAAT |
| *MAP1LC3A* | GTGAACCAGCACAGCAT | GGAGGCGTAGACCATATAGA |
| *ATG5* | AGCAACTCTGGATGGGATTG | AGGTCTTTCAGTCGTTGTCTG |
| *BECN1* | AAGAGGTTGAGAAAGGCGAG | TGGGTTTTGATGGAATAGGAGC |
| *SQSTM1* | AATCAGCTTCTGGTCCATCG | TTCTTTTCCCTCCGTGCTC |
| *STAMP2* | CTTGGTAGCTCTGGGATTTG | GAGAATCCATTTAGCACCTCC |
| *GAPDH* | GTCAGTGGTGGACCTGACCT | TCGCTGTTGAAGTCAGAGGA |
| *ACTB* | GGCTACAGCTTCACCACCAC | GTCAGGCAGCTCGTAGCTCT |
| *TBP* | GAGCTGTGATGTGAAGTTTCC | TCTGGGTTTGATCATTCTGTA |
| *NPC1* | GCCTACCGAGTATTTCCTTAC | CACACCGAGGTTGAAGATAG |
| *MCOLN1* | TCTCCCAGCTCTACCTTTAC | GATGCTTGATGGTGTCGTAG |
| *ATG5* | AGCAACTCTGGATGGGATTG | AGGTCTTTCAGTCGTTGTCTG |

**Long-lived protein degradation**

LNCaP cells were seeded into 24 well plates at a density of $0.7 - 1.0 * 10^5$ cells/ml. Each condition was replicated three times for statistical analysis. $10^{-8}$M R1881 (synthetic androgen) was added to the cell suspension to induce the expression of STAMP2 and to replicate physiological conditions of the prostate. $^{14}$C-L-Valine (10 mM) was supplemented to the cell suspension to incorporate radioactivity to newly synthesized proteins. After seeding, the cells were left to incubate for 48 hours at 37$^o$C to incorporate $^{14}$C-L-Valine into newly synthesized

proteins. After the 48-hour incubation, the radioactive cell medium was removed and every well was washed in warm culture medium. 400 µl culture media supplemented with L-Valine (10 mM) (referred henceforth as RPMI-Val/EBSS-Val) was then replenished into each well. The plates are left for 24 hours in the RPMI-Val at 37°C to remove radioactively labelled short-lived proteins. The chase media are removed and the wells were washed with 300 µl of EBSS-Val for starvation condition cells and RPMI-Val for fed condition cells. The starvation condition cells were starved with EBSS-Val in the presence/absence of 100 nM Bafilomycin for 4 hours. Fed condition cells were incubated in full RPMI-Val supplemented with/without 100 nM Bafilomycin for 4 hours.

After 4 hours, the medium of the samples were collected into Eppendorf tubes. The wells were washed with 70 µl 1% BSA and the BSA was transferred into the tubes containing the supernatant. Into each tube, 70µl 50 % TCA was added and the tubes were kept for 24 hours at 4°C. 400 µl 0.2 M KOH was then added to each well and kept at 4°C for 24 hours. The supernatant fraction and pellet fraction was dissolved in UltimaGold liquid scintillation cocktail, and radioactivity was analyzed on a liquid scintillation counter.

**Immunofluorescence microscopy**

Cells were seeded in 24 well plates containing glass cover slips. Following the respective treatments, the cells were washed twice in PBS and fixed in 4% PFA (pH 7.2) for 15 minutes. The fixed cells were then washed twice in PBS and incubated with DMEM (10mM HEPES pH7.4) for 10 minutes. The cells were then incubated in blocking buffer (PBS, 5% BSA and 0.05% saponin) for 30 minutes. After blocking, primary antibodies diluted in blocking buffer were added to the cells for 1 hour at room temperature. The cover slips were washed in PBS and incubated in secondary antibody diluted in blocking buffer for 45 minutes at RT. The cells were washed twice with PBS and cell nuclei was stained using DAPI (0.3 µg/ml) in PBS for 5 minutes at RT. The cells were then washed with distilled water and mounted with Mowiol on microscope slides.

**Fluorescence microscopy**

siRNA- or shRNA-treated LNCaP cells were grown on sterilized glass coverslips in 24 well dishes. The cells were starved or not for 2 hours in the presence or absence of Bafilomycin A1 (100nM), washed twice in ice cold PBS and fixed in 4% paraformaldehyde (PFA) for 15 minutes at room temperature. The nuclei were counterstained with 0.3 µg/ml DAPI in PBS for

5 minutes at room temperature. Fluorescence was observed using an ULSAPO 40-X objective attached to an automated Olympus ScanR microscope. Fluorescence was quantified using the physiology module included in the Zeiss Assaybuilder program.

**Lentivirus transduction and stable cell line selection**

HEK293T cells were transfected with lentivirus plasmids using the ThermoScientific Trans-Lentiviral Packaging Kit (TLP5913). 64 hours post transfection, the media containing lentivirus was collected and passed through a sterile filter. LNCaP cells to be transduced were then incubated in the lentivirus containing media for 4 hours. The media was then removed and the cells were incubated for 48 hours, and selected using 1µg/ml puromycin for 2 weeks. The cells were then maintained in media containing 0.2µg/ml puromycin to maintain selection pressure. The knockdown efficiency was determined by qPCR.

**Subcellular fractionation**

Subcellular fractionation was carried out using the ThermoScientific Subcellular Protein Fractionation Kit for Cultured cells (#78840) according to manufacturer's instructions. In short, the siRNA treated cells were grown in 10cm dishes, after which washed with ice cold PBS and treated according to manufacturer's instructions.

**Bioinformatic analyses**

The correlation between STAMP2 and LC3 family gene expression in PCa was conducted with RNA sequencing data from the cancer genome atlas study (171) The population of STAMP2 expressing samples were stratified from the median into two populations based on STAMP2 expression and plotted in Microsoft Excel.

**Microarray**

The microarray gene expression analysis was performed at the Radium hospital. LNCaP cells treated with control or STAMP2 siRNA in the presence or absence of 10 nM R1881 for 48 hours were analysed by microarray for gene expression profiling. A bioanalyzer was used to determine RNA integrity. Samples with RNA integrity number (RIN) greater than 7 were selected for downstream analysis. The RNA was amplified and hybridized to Illumina HumanHT-12 v4 arrays. A cutoff of 1.2 fold expression change was used to determine gene upregulations.

**Statistics**

All error bars represent standard deviation. Unless specified, p-values were derived from two-tailed, two-sample Student's t-test using Microsoft Excel, and considered statistically significant only when $p < 0.05$.

# 4   Summary of results

The results presented in Paper I describes the involvement of STAMP2 in regulating autophagy in PCa cells. In a previous study conducted in our lab, we show that STAMP2 is an oncogenic driver of PCa in both *in vitro* and *in vivo* settings. However, the exact role of STAMP2 in homeostatic maintenance in the cell remains to be investigated. The data obtained in the present study is presented in Paper I entitled "The role of STAMP2 in the regulation of autophagy in prostate Cancer cells."

**Autophagic flux.** Upon STAMP2 depletion by siRNA mediated knockdown, LC3 lipidation and puncta formation increased in LNCaP cells. STAMP2 knockdown led to increased PE conjugated form of LC3 (LC3-II), which is closely correlated to the amount of autophagosomes in the cell (172). This accumulation was found to be caused by increased autophagic flux as inhibition of the autophagy using the lysosomal V-ATPase Bafilomycin A1 (BafA1) induced further accumulation of LC3-II and LC3 puncta formation. Conversely, ectopic expression of STAMP2 decreased LC3-II formation, indicating that STAMP2 represses autophagy. Consistent with the previous hypothesis, long-lived protein degradation in the lysosomes were also increased upon the STAMP2 knockdown.

**ULK1 activation.** Autophagy initiation is regulated by the ULK complex, which is itself regulated by phosphorylation by its activator, AMPK and its repressor, mTOR. We sought to investigate if STAMP2 levels regulates autophagy in its early stages, and found that ULK1 activating phosphorylation was increased upon STAMP2 knockdown, while inhibitory ULK1 phosphorylation was decreased.

**Gene expression changes.** The increase in total LC3 upon STAMP2 knockdown suggested transcriptional reprogramming of autophagy genes. STAMP2 knockdown induced the upregulation of *LC3b* and *SQSTM1*, while the overexpression of STAMP2 repressed transcription of the autophagy genes. We wanted to investigate if this observation is also seen in the cancer patients. Analysis of clinical data showed that the expression of *SQSTM1* and every member of the LC3 family of proteins, except *GABARAPL1* is increased in tumors with lower STAMP2 expression.

**TFEB activation.** To identify the transcription factor responsible for this upregulation of autophagy, we performed microarray analysis to identify the group of genes that are altered

upon STAMP2 knockdown. TFEB target genes were found to be enriched upon STAMP2 depletion. To follow up on this, we looked at the TFEB activation by comparing the nuclear presence of TFEB in STAMP2 knockdown and control cells. Nuclear TFEB was increased in the nucleus in both fed and starved states, indicating that STAMP2 is able to regulate TFEB activation.

# 5  Discussion and future perspectives

The main goal of this thesis is to investigate the potential involvement of STAMP2 in autophagy in PCa cells and to unravel the possible mechanisms behind it. We initially asked whether STAMP2 could represent a novel autophagy-regulating protein given that it is an important survival factor in PCa. The results presented in Paper I reveal a novel role for STAMP2 in repressing autophagy in PCa cells, at least in part, through regulation of early autophagy signaling events and changes in Atg gene transcription.

To study the autophagic flux, we employed LC3 lipidation assays, LC3 puncta formation studies and long-lived protein analysis (173). The amount of PE conjugated LC3 (LC3-II) is directly correlated to the number of autophagosomes in the cell. LC3-II abundance can be studied by western blotting and by counting LC3 puncta during immunofluorescence microscopy. LC3 lipidation and puncta formation is increased when STAMP2 is depleted, and was conversely decreased when STAMP2 is overexpressed. These findings suggest that autophagosome formation may be inhibited by STAMP2. In order to study this, further experiments such as electron microscopy analysis are required. Interestingly, in contrast to the obvious increase in LC3-I levels in STAMP2 knockdown cells, LC3-I levels were not lowered in LNCaP cells overexpressing STAMP2. This indicates that several different mechanism may be involved in repressing and activating autophagy when STAMP2 levels are altered.

The early stages of autophagy initiation is regulated by both the ULK and PI3K complexes (174). The ULK complex, which is necessary for recruitment of Atg proteins to the growing phagophore, is activated by increased phosphorylation on serine residues by AMPK or is repressed by mTOR-mediated phosphorylation (63, 65). The loss of STAMP2 activated the ULK complex, as assessed by the increase of the activating serine phosphorylation at S555 and decrease of the repressive serine phosphorylation at S757. Because ULK1 activation leads to recruitment of Atg proteins to the growing phagophore (42), we would therefore expect increased 1000phagophore formation. To follow up on this, we are currently studying the formation of ATG5, ATG16L1 and WIPI2 puncta that functions as markers of the phagophore. The increase in mTOR activation upon STAMP2 loss is, however, puzzling as mTOR is a known repressor of autophagosome formation (65). However, p70S6K phosphorylation does not always correspond to inhibition of autophagy (175). Thus, in addition to p70S6K, another readout of mTOR activation, such as phospho-4-EBP1 or mTOR-lysosome colocalization

should be used in future experiments. Unfortunately due to difficulties in observing phosphorylated AMPK on western analysis with the antibody currently available to us, we were unable to confirm changes to AMPK activation when STAMP2 levels are altered, despite changes to AMPK dependent ULK1 phosphorylation sites. The activation of AMPK needs to be studied further given its direct role in ULK activation.

Autophagy can be transcriptionally regulated by a multiple array of transcription factors (176). The increase in LC3-I protein levels upon STAMP2 knockdown suggests that LC3 is transcriptionally upregulated. We therefore asked if autophagy gene expression is altered by STAMP2. The expression of multiple autophagy genes was increased by STAMP2 depletion, while STAMP2 overexpression repressed autophagy gene expression. For example, we observed that *MAP1LC3b* and *SQSTM1* mRNA was increased upon STAMP2 knockdown and was decreased when STAMP2 was overexpressed. Because the transcription factor ATF4 is regulated by STAMP2 (149), we included its target genes, ATG5 and BECN1, in the RT-qPCR analysis. ATF4 regulated autophagy genes (75) were not upregulated when STAMP2 was lost. *ATG5* and *BECN1* expression was not altered when STAMP2 was lost, indicating that ATF4 might not be the transcription factor responsible for the increase in LC3 and p62 protein levels during autophagy in PCa cells.

Every member of the LC3 family, except *GABARAPL1* was upregulated in a PCa cohort with low STAMP2 expression. This suggests that the transcriptional upregulation we observed in *in vitro* cell culture experiments extends to *in situ* disease. Immunohistochemistry (IHC) analysis of patient tumor samples should be investigated to study whether the increase in gene expression leads to increased autophagy proteins. Additionally, IHC analysis lipidated LC3 and STAMP2 in clinical samples needs to be assessed to validate the relationship between STAMP2 and autophagy in PCa.

cDNA microarray analysis showed that multiple TFEB target genes were increased in STAMP2 knockdown cells, and cellular fractionation assays showed that TFEB was primarily nuclear when STAMP2 was depleted. These events, in addition to increased lysosome number in STAMP2 knocked down cells, suggest that TFEB was activated. Chromatin immunoprecipitation experiments may be utilized to validate the binding and activation of Atg promoter sequences and luciferase based promoter assays can be used to study the activation of Atg gene promoters. The next piece of the puzzle would be a mechanistic explanation to describe how STAMP2 is controlling TFEB activation. One hypothesis is that STAMP2 may

alter intracellular calcium levels, an event that controls TFEB activation (89). Preliminary data suggests that the ER calcium storage and the endolysosomal calcium channel Mucolipin-1 (MCOLN1) may be involved.

Global gene expression analysis show that genes involved in lysosome function is upregulated when STAMP2 is lost, among them genes involved in lysosomal acidification. The lysosomes regulate their pH levels through V-type ATPases that are necessary for amino acid-based mTORC1 activation (177), and increased $H^+$ ions may increase the positive charge in the lysosomal lumen and thus alter lysosomal membrane potential. It is therefore relevant to investigate if lysosomal pH is altered upon STAMP2 knockdown, possibly by quantification of lysotracker staining intensity.

The experiments conducted in Paper I were done in LNCaP and VCaP cells. Experiments should eventually be extended to additional PCa cell lines, for example, 22RV1 and PC-3, to confirm that the effects of STAMP2 on autophagy are not cell line specific observations. Broadening the investigation to include cell lines derived from different organs and organisms would further support a general functional association between STAMP and autophagy. Investigation of cell lines originating from the liver, which is regarded to have both high autophagic flux and high STAMP2 expression (152), could provide a model for studying the relationship between STAMP2 and autophagy.

The repression of autophagy by STAMP2 could possibly be caused by inhibition of autophagosome-lysosome fusion. To confirm this, we are currently generating stable PCa cell lines expressing mCherry-EGFP-LC3b. As EGFP is more sensitive towards the low pH compared to mCherry, EGFP is quenched in the acidic environment of the lysosomes while the mCherry signal remains visible (178). Thus, observing the shift of mCherry[(+)]-EGFP[(+)]-LC3b (Yellow) puncta to mCherry[(+)]-EGFG[(-)]-LCb (Red) puncta will allow us to quantitatively validate the maturation of autophagosomes into autolysosomes.

The V-type ATPase inhibitory properties BafA1 (179) was used in this thesis to inhibit lysosomal degradation. Since STAMP2 induces differences in gene expression of lysosomal genes, cells with differing levels of STAMP2 could have different predisposition to the inhibitor, thus providing inaccurate assessment of the autophagic flux. To control for this, we should employ the use of additional autophagy inhibitors, such as cathepsin inhibitors (E-64d) or PI3K inhibitors (3-Methyladenine (3-MA) or Wortmannin). Autophagy comprises of

multiple stages, from initiation, nucleation and fusion with lysosomes. By employing different autophagy inhibitors to block autophagy at different stages of its progression, we will be able to hone in on complexes or processes that STAMP2 may potentially influence. 3-MA inhibit autophagy initiation by preventing PI3P generation (180). If differences to LC3 lipidation is observed already after 3-MA treatment, we could assume that STAMP2 affects early autophagic events, which would suggest further investigations into the PI3K complex or ULK1 complex. Conversely, if no changes are observed after 3-MA, we may infer that STAMP2 might regulate later stages of autophagy.

Improved understanding of STAMP2 biology could aid in better understanding its role in autophagy. GFP-tagged STAMP2 has been observed in the ER and early endosomal compartments (141). However, the presence of an additional 27 kDa fluorophore could possibly alter the normal behavior and transport of STAMP2. Unfortunately, due the absence of reliable antibodies against STAMP2, we are at present unable to detect the localization of endogenous STAMP2. The optimal NADPH oxidase activity of STAMP2 is obtained in the range of pH 5-5.5 (137), which is close to the pH of the lysosomal lumen. This would suggest that STAMP2 may have potential functions in the lysosomes and may affect autophagy there. Furthermore, the interplay between STAMP1, STAMP2 and STAMP3 remains poorly understood. Given the high sequence similarity that the STAMPs share (132), STAMP1 and STAMP3 could also be involved in regulating autophagy in addition to STAMP2. Simultaneous knockdown of multiple STAMPs could show if the STAMPs are redundant, or if members of the STAMP family have individual specific roles in autophagy.

The close association of STAMP2 to endosomal compartments suggests that it may play roles in membrane trafficking events, such as endocytosis and/or secretion (141). Autophagy is a membrane trafficking event in the cells that leads to the breakdown of cellular material in the lysosomes, which is now accepted to play active roles in carcinogenesis (181). In PCa, autophagy is seen to be protective towards unfavorable conditions such as low androgen levels or starvation of PCa cells. The numerous roles that STAMP2 play in cellular differentiation (139, 170), inflammation (159), insulin signaling (168) and iron uptake (131) suggests that its loss or upregulation may affect homeostasis. This led us to question the role of STAMP2 in the cell. For example, mitophagy is induced upon iron depletion (182), would then the loss of STAMP2, an iron reductase, have any effects on this mitochondrial degradation? Previous studies have shown accumulation of damaged mitochondria when cells are treated with anti-STAMP2 antibodies (183, 184), suggesting that STAMP2 inhibtion may induce mitochondria

damage or that mitophagy may be compromised. Thus, the relationship between mitochondria degradation and STAMP2 should be investigated.

Many questions remain concerning the exact function that STAMP2 plays in autophagy. Are the functional domains of STAMP2 required for the observed effects on autophagy? The NADPH oxidase domain is involved in the generation of ROS, which is capable of both activating and repressing autophagy (185). Antioxidants can utilized to remove intracellular ROS to examine the relevance of the ROS generated by STAMP2 in autophagy. Moreover, previous studies have indicated that cellular iron levels regulate HIF1α signaling (186) and mitophagy (182).Given that STAMP2 may be involved in transferrin dependent iron uptake (135), it would be of interest to see if iron levels are altered in PCa by the ferrireductase domain of STAMP2 and to see if this induces HIF1α dependent autophagy or mitophagy. Thus, mutation studies of STAMP2 domains are currently underway to see which STAMP2 region is required for autophagy regulation.

Given that autophagy promotes therapeutic resistance and is a survival factor in multiple cancers including PCa (124, 187), low amounts of STAMP2 could possibly be an indication of increased treatment survival and drug resistance. One possible way of studying this is to challenge STAMP2 knockdown cells with ADT. This further raises the possibility that STAMP2 expression profiles could be used as an additional factor in predicting ADT response in PCa. Alternatively, PCa tumors with low STAMP2 expression, corresponding to increased autophagy activation, would possibly benefit from combinatorial treatments with autophagy inhibitors. The results of this study might thus contribute towards better understanding of PCa cell biology and may provide novel approaches to detect and target this disease.

# 6 References

1.    Abate-Shen C, Shen MM. Molecular genetics of prostate cancer. Genes & development. 2000;14(19):2410-34.
2.    McNeal JE. Normal histology of the prostate. The American journal of surgical pathology. 1988;12(8):619-33.
3.    Shen MM, Abate-Shen C. Molecular genetics of prostate cancer: new prospects for old challenges. Genes & development. 2010;24(18):1967-2000.
4.    Martini FH TM, Tallitsch RB. Human anatomy. Cummings PB, editor. San Francisco: Pearson Benjamin Cummings; 2012.
5.    Sheir D, Butler and Lewis, R. Hole's Essentials of Human Anatomy and Physiology. Hill WM, editor. Boston1988.
6.    Bray F, Jemal A, Grey N, Ferlay J, Forman D. Global cancer transitions according to the Human Development Index (2008-2030): a population-based study. The Lancet Oncology. 2012;13(8):790-801.
7.    Siegel R, Naishadham D, Jemal A. Cancer statistics, 2013. CA: a cancer journal for clinicians. 2013;63(1):11-30.
8.    Cancer-Registry N. Cancer in Norway 2015; Cancer incidence, mortality, survival and prevalence in Norway. Research IoPBC; 2016.
9.    Deutsch E, Maggiorella L, Eschwege P, Bourhis J, Soria JC, Abdulkarim B. Environmental, genetic, and molecular features of prostate cancer. The Lancet Oncology. 2004;5(5):303-13.
10.   Hsing AW, Chokkalingam AP. Prostate cancer epidemiology. Frontiers in bioscience : a journal and virtual library. 2006;11:1388-413.
11.   Parkin DM, Bray F, Ferlay J, Pisani P. Global Cancer Statistics, 2002. CA: a cancer journal for clinicians. 2005;55(2):74-108.
12.   Powell IJ. Epidemiology and pathophysiology of prostate cancer in African-American men. The Journal of urology. 2007;177(2):444-9.
13.   Hill P, Wynder EL, Garbaczewski L, Garnes H, Walker AR. Diet and urinary steroids in black and white North American men and black South African men. Cancer research. 1979;39(12):5101-5.
14.   Hubbard JS, Rohrmann S, Landis PK, Metter EJ, Muller DC, Andres R, et al. Association of prostate cancer risk with insulin, glucose, and anthropometry in the Baltimore longitudinal study of aging. Urology. 2004;63(2):253-8.
15.   Huncharek M, Haddock KS, Reid R, Kupelnick B. Smoking as a Risk Factor for Prostate Cancer: A Meta-Analysis of 24 Prospective Cohort Studies. American Journal of Public Health. 2010;100(4):693-701.
16.   Bostwick DG, Burke HB, Djakiew D, Euling S, Ho SM, Landolph J, et al. Human prostate cancer risk factors. Cancer. 2004;101(10 Suppl):2371-490.
17.   Ferguson J, Zincke H, Ellison E, Bergstrahl E, Bostwick DG. Decrease of prostatic intraepithelial neoplasia following androgen deprivation therapy in patients with stage T3 carcinoma treated by radical prostatectomy. Urology. 1994;44(1):91-5.
18.   Shappell SB, Thomas GV, Roberts RL, Herbert R, Ittmann MM, Rubin MA, et al. Prostate pathology of genetically engineered mice: definitions and classification. The consensus report from the Bar Harbor meeting of the Mouse Models of Human Cancer Consortium Prostate Pathology Committee. Cancer research. 2004;64(6):2270-305.
19.   Cheng L, Montironi R, Bostwick DG, Lopez-Beltran A, Berney DM. Staging of prostate cancer. Histopathology. 2012;60(1):87-117.

20.     Abeshouse A, Ahn J, Akbani R, Ally A, Amin S, Andry Christopher D, et al. The Molecular Taxonomy of Primary Prostate Cancer. Cell. 2015;163(4):1011-25.

21.     Yuan X, Cai C, Chen S, Chen S, Yu Z, Balk SP. Androgen receptor functions in castration-resistant prostate cancer and mechanisms of resistance to new agents targeting the androgen axis. Oncogene. 2014;33(22):2815-25.

22.     Karantanos T, Corn PG, Thompson TC. Prostate cancer progression after androgen deprivation therapy: mechanisms of castrate resistance and novel therapeutic approaches. Oncogene. 2013;32(49):5501-11.

23.     Kaur J, Debnath J. Autophagy at the crossroads of catabolism and anabolism. Nat Rev Mol Cell Biol. 2015;16(8):461-72.

24.     Kunz JB, Schwarz H, Mayer A. Determination of Four Sequential Stages during Microautophagy in Vitro. Journal of Biological Chemistry. 2004;279(11):9987-96.

25.     Fred Dice J. Peptide sequences that target cytosolic proteins for lysosomal proteolysis. Trends in Biochemical Sciences. 1990;15(8):305-9.

26.     Chiang H, Terlecky, Plant C, Dice J. A role for a 70-kilodalton heat shock protein in lysosomal degradation of intracellular proteins. Science (New York, NY). 1989;246(4928):382-5.

27.     Axe EL, Walker SA, Manifava M, Chandra P, Roderick HL, Habermann A, et al. Autophagosome formation from membrane compartments enriched in phosphatidylinositol 3-phosphate and dynamically connected to the endoplasmic reticulum. The Journal of Cell Biology. 2008;182(4):685-701.

28.     Ravikumar B, Moreau K, Jahreiss L, Puri C, Rubinsztein DC. Plasma membrane contributes to the formation of pre-autophagosomal structures. Nat Cell Biol. 2010;12(8):747-57.

29.     Hailey DW, Rambold AS, Satpute-Krishnan P, Mitra K, Sougrat R, Kim PK, et al. Mitochondria supply membranes for autophagosome biogenesis during starvation. Cell. 2010;141(4):656-67.

30.     Geng J, Nair U, Yasumura-Yorimitsu K, Klionsky DJ. Post-Golgi Sec proteins are required for autophagy in Saccharomyces cerevisiae. Molecular biology of the cell. 2010;21(13):2257-69.

31.     Lazarou M, Sliter DA, Kane LA, Sarraf SA, Wang C, Burman JL, et al. The ubiquitin kinase PINK1 recruits autophagy receptors to induce mitophagy. Nature. 2015;524(7565):309-14.

32.     Park YE, Hayashi YK, Bonne G, Arimura T, Noguchi S, Nonaka I, et al. Autophagic degradation of nuclear components in mammalian cells. Autophagy. 2009;5(6):795-804.

33.     Maejima I, Takahashi A, Omori H, Kimura T, Takabatake Y, Saitoh T, et al. Autophagy sequesters damaged lysosomes to control lysosomal biogenesis and kidney injury. Embo j. 2013;32(17):2336-47.

34.     Papadopoulos C, Kirchner P, Bug M, Grum D, Koerver L, Schulze N, et al. VCP/p97 cooperates with YOD1, UBXD1 and PLAA to drive clearance of ruptured lysosomes by autophagy. The EMBO Journal. 2017;36(2):135-50.

35.     Yokota S. Degradation of normal and proliferated peroxisomes in rat hepatocytes: regulation of peroxisomes quantity in cells. Microscopy research and technique. 2003;61(2):151-60.

36.     Bernales S, Schuck S, Walter P. ER-phagy: selective autophagy of the endoplasmic reticulum. Autophagy. 2007;3(3):285-7.

37.     Yuk J-M, Yoshimori T, Jo E-K. Autophagy and bacterial infectious diseases. Exp Mol Med. 2012;44:99-108.

38.     Hyttinen JM, Amadio M, Viiri J, Pascale A, Salminen A, Kaarniranta K. Clearance of misfolded and aggregated proteins by aggrephagy and implications for aggregation diseases. Ageing research reviews. 2014;18:16-28.

39.     Wesselborg S, Stork B. Autophagy signal transduction by ATG proteins: from hierarchies to networks. Cellular and Molecular Life Sciences. 2015;72:4721-57.

40.     Young AR, Chan EY, Hu XW, Kochl R, Crawshaw SG, High S, et al. Starvation and ULK1-dependent cycling of mammalian Atg9 between the TGN and endosomes. Journal of cell science. 2006;119(Pt 18):3888-900.

41.     Chan EY, Longatti A, McKnight NC, Tooze SA. Kinase-inactivated ULK proteins inhibit autophagy via their conserved C-terminal domains using an Atg13-independent mechanism. Molecular and cellular biology. 2009;29(1):157-71.

42.     Karanasios E, Stapleton E, Manifava M, Kaizuka T, Mizushima N, Walker SA, et al. Dynamic association of the ULK1 complex with omegasomes during autophagy induction. Journal of cell science. 2013;126(Pt 22):5224-38.

43.     Itakura E, Mizushima N. Atg14 and UVRAG: mutually exclusive subunits of mammalian Beclin 1-PI3K complexes. Autophagy. 2009;5(4):534-6.

44.     Dooley Hannah C, Razi M, Polson Hannah E, Girardin Stephen E, Wilson Michael I, Tooze Sharon A. WIPI2 Links LC3 Conjugation with PI3P, Autophagosome Formation, and Pathogen Clearance by Recruiting Atg12–5-16L1. Molecular Cell. 2014;55(2):238-52.

45.     Polson HE, de Lartigue J, Rigden DJ, Reedijk M, Urbe S, Clague MJ, et al. Mammalian Atg18 (WIPI2) localizes to omegasome-anchored phagophores and positively regulates LC3 lipidation. Autophagy. 2010;6(4):506-22.

46.     Fujita N, Itoh T, Omori H, Fukuda M, Noda T, Yoshimori T. The Atg16L complex specifies the site of LC3 lipidation for membrane biogenesis in autophagy. Molecular biology of the cell. 2008;19(5):2092-100.

47.     Puri C, Renna M, Bento CF, Moreau K, Rubinsztein DC. Diverse autophagosome membrane sources coalesce in recycling endosomes. Cell. 2013;154(6):1285-99.

48.     Mizushima N, Noda T, Yoshimori T, Tanaka Y, Ishii T, George MD, et al. A protein conjugation system essential for autophagy. Nature. 1998;395(6700):395-8.

49.     Ohsumi Y, Mizushima N. Two ubiquitin-like conjugation systems essential for autophagy. Seminars in cell & developmental biology. 2004;15(2):231-6.

50.     Gammoh N, Florey O, Overholtzer M, Jiang X. Interaction Between FIP200 and ATG16L1 Distinguishes ULK1 Complex-Dependent and -Independent Autophagy. Nature structural & molecular biology. 2013;20(2):144-9.

51.     Satoo K, Noda NN, Kumeta H, Fujioka Y, Mizushima N, Ohsumi Y, et al. The structure of Atg4B–LC3 complex reveals the mechanism of LC3 processing and delipidation during autophagy. The EMBO Journal. 2009;28(9):1341-50.

52.     Shpilka T, Weidberg H, Pietrokovski S, Elazar Z. Atg8: an autophagy-related ubiquitin-like protein family. Genome Biology. 2011;12(7):226.

53.     Fujita N, Itoh T, Omori H, Fukuda M, Noda T, Yoshimori T. The Atg16L Complex Specifies the Site of LC3 Lipidation for Membrane Biogenesis in Autophagy. Molecular biology of the cell. 2008;19(5):2092-100.

54.     Birgisdottir AB, Lamark T, Johansen T. The LIR motif - crucial for selective autophagy. Journal of cell science. 2013;126(Pt 15):3237-47.

55.     Johansen T, Lamark T. Selective autophagy mediated by autophagic adapter proteins. Autophagy. 2011;7(3):279-96.

56.     Martin DDO, Ladha S, Ehrnhoefer DE, Hayden MR. Autophagy in Huntington disease and huntingtin in autophagy. Trends in Neurosciences. 2015;38(1):26-35.

57.     Lynch-Day MA, Mao K, Wang K, Zhao M, Klionsky DJ. The Role of Autophagy in Parkinson's Disease. Cold Spring Harbor Perspectives in Medicine. 2012;2(4):a009357.

58.	Kirisako T, Ichimura Y, Okada H, Kabeya Y, Mizushima N, Yoshimori T, et al. The reversible modification regulates the membrane-binding state of Apg8/Aut7 essential for autophagy and the cytoplasm to vacuole targeting pathway. Journal of Cell Biology. 2000;151(2):263-75.

59.	Ravikumar B, Acevedo-Arozena A, Imarisio S, Berger Z, Vacher C, O'Kane CJ, et al. Dynein mutations impair autophagic clearance of aggregate-prone proteins. Nature genetics. 2005;37(7):771-6.

60.	Maday S, Wallace KE, Holzbaur EL. Autophagosomes initiate distally and mature during transport toward the cell soma in primary neurons. J Cell Biol. 2012;196(4):407-17.

61.	Itakura E, Kishi-Itakura C, Mizushima N. The hairpin-type tail-anchored SNARE syntaxin 17 targets to autophagosomes for fusion with endosomes/lysosomes. Cell. 2012;151(6):1256-69.

62.	Diao J, Liu R, Rong Y, Zhao M, Zhang J, Lai Y, et al. ATG14 promotes membrane tethering and fusion of autophagosomes to endolysosomes. Nature. 2015;520(7548):563-6.

63.	Alers S, Löffler AS, Wesselborg S, Stork B. Role of AMPK-mTOR-Ulk1/2 in the Regulation of Autophagy: Cross Talk, Shortcuts, and Feedbacks. Molecular and cellular biology. 2012;32(1):2-11.

64.	Efeyan A, Comb WC, Sabatini DM. Nutrient Sensing Mechanisms and Pathways. Nature. 2015;517(7534):302-10.

65.	Kim J, Kundu M, Viollet B, Guan KL. AMPK and mTOR regulate autophagy through direct phosphorylation of Ulk1. Nat Cell Biol. 2011;13(2):132-41.

66.	Burman C, Ktistakis NT. Regulation of autophagy by phosphatidylinositol 3-phosphate. FEBS letters. 2010;584(7):1302-12.

67.	Stenmark H, Aasland R, Driscoll PC. The phosphatidylinositol 3-phosphate-binding FYVE finger. FEBS letters. 2002;513(1):77-84.

68.	Proikas-Cezanne T, Waddell S, Gaugel A, Frickey T, Lupas A, Nordheim A. WIPI-1[alpha] (WIPI49), a member of the novel 7-bladed WIPI protein family, is aberrantly expressed in human cancer and is linked to starvation-induced autophagy. Oncogene. 2004;23(58):9314-25.

69.	Chantranupong L, Scaria SM, Saxton RA, Gygi MP, Shen K, Wyant GA, et al. The CASTOR Proteins Are Arginine Sensors for the mTORC1 Pathway. Cell. 2016;165(1):153-64.

70.	Rebsamen M, Pochini L, Stasyk T, de Araujo MEG, Galluccio M, Kandasamy RK, et al. SLC38A9 is a component of the lysosomal amino acid sensing machinery that controls mTORC1. Nature. 2015;519(7544):477-81.

71.	Sancak Y, Bar-Peled L, Zoncu R, Markhard AL, Nada S, Sabatini DM. Ragulator-Rag complex targets mTORC1 to the lysosomal surface and is necessary for its activation by amino acids. Cell. 2010;141(2):290-303.

72.	Fumagalli F, Noack J, Bergmann TJ, Presmanes EC, Pisoni GB, Fasana E, et al. Translocon component Sec62 acts in endoplasmic reticulum turnover during stress recovery. Nat Cell Biol. 2016;18(11):1173-84.

73.	Ogata M, Hino S, Saito A, Morikawa K, Kondo S, Kanemoto S, et al. Autophagy is activated for cell survival after endoplasmic reticulum stress. Molecular and cellular biology. 2006;26(24):9220-31.

74.	Margariti A, Li H, Chen T, Martin D, Vizcay-Barrena G, Alam S, et al. XBP1 mRNA Splicing Triggers an Autophagic Response in Endothelial Cells through BECLIN-1 Transcriptional Activation. Journal of Biological Chemistry. 2013;288(2):859-72.

75.	B'Chir W, Maurin AC, Carraro V, Averous J, Jousse C, Muranishi Y, et al. The eIF2alpha/ATF4 pathway is essential for stress-induced autophagy gene expression. Nucleic acids research. 2013;41(16):7683-99.

76.     Pike LR, Singleton DC, Buffa F, Abramczyk O, Phadwal K, Li JL, et al. Transcriptional up-regulation of ULK1 by ATF4 contributes to cancer cell survival. The Biochemical journal. 2013;449(2):389-400.

77.     Milani M, Rzymski T, Mellor HR, Pike L, Bottini A, Generali D, et al. The role of ATF4 stabilization and autophagy in resistance of breast cancer cells treated with Bortezomib. Cancer research. 2009;69(10):4415-23.

78.     Zhu G, Wu CJ, Zhao Y, Ashwell JD. Optineurin negatively regulates TNFalpha-induced NF-kappaB activation by competing with NEMO for ubiquitinated RIP. Current biology : CB. 2007;17(16):1438-43.

79.     Yu HB, Kielczewska A, Rozek A, Takenaka S, Li Y, Thorson L, et al. Sequestosome-1/p62 Is the Key Intracellular Target of Innate Defense Regulator Peptide. Journal of Biological Chemistry. 2009;284(52):36007-11.

80.     Hiruma Y, Kurihara N, Subler MA, Zhou H, Boykin CS, Zhang H, et al. A SQSTM1/p62 mutation linked to Paget's disease increases the osteoclastogenic potential of the bone microenvironment. Human molecular genetics. 2008;17(23):3708-19.

81.     Jin Z, Li Y, Pitti R, Lawrence D, Pham VC, Lill JR, et al. Cullin3-based polyubiquitination and p62-dependent aggregation of caspase-8 mediate extrinsic apoptosis signaling. Cell. 2009;137(4):721-35.

82.     Lee HK, Lund JM, Ramanathan B, Mizushima N, Iwasaki A. Autophagy-dependent viral recognition by plasmacytoid dendritic cells. Science (New York, NY). 2007;315(5817):1398-401.

83.     Lee JM, Wagner M, Xiao R, Kim KH, Feng D, Lazar MA, et al. Nutrient-sensing nuclear receptors coordinate autophagy. Nature. 2014;516(7529):112-5.

84.     Copetti T, Bertoli C, Dalla E, Demarchi F, Schneider C. p65/RelA Modulates BECN1 Transcription and Autophagy. Molecular and cellular biology. 2009;29(10):2594-608.

85.     Seok S, Fu T, Choi SE, Li Y, Zhu R, Kumar S, et al. Transcriptional regulation of autophagy by an FXR-CREB axis. Nature. 2014;516(7529):108-11.

86.     Settembre C, Di Malta C, Polito VA, Arencibia MG, Vetrini F, Erdin S, et al. TFEB Links Autophagy to Lysosomal Biogenesis. Science (New York, NY). 2011;332(6036):1429-33.

87.     Martina JA, Chen Y, Gucek M, Puertollano R. MTORC1 functions as a transcriptional regulator of autophagy by preventing nuclear transport of TFEB. Autophagy. 2012;8(6):903-14.

88.     Yang D, Holt GE, Velders MP, Kwon ED, Kast WM. Murine six-transmembrane epithelial antigen of the prostate, prostate stem cell antigen, and prostate-specific membrane antigen: prostate-specific cell-surface antigens highly expressed in prostate cancer of transgenic adenocarcinoma mouse prostate mice. Cancer research. 2001;61(15):5857-60.

89.     Medina DL, Di Paola S, Peluso I, Armani A, De Stefani D, Venditti R, et al. Lysosomal calcium signalling regulates autophagy through calcineurin and TFEB. Nat Cell Biol. 2015;17(3):288-99.

90.     White E, DiPaola RS. The Double-edged Sword of Autophagy Modulation in Cancer. Clinical cancer research : an official journal of the American Association for Cancer Research. 2009;15(17):5308-16.

91.     Liou G-Y, Storz P. Reactive oxygen species in cancer. Free radical research. 2010;44(5):10.3109/10715761003667554.

92.     Kansanen E, Kuosmanen SM, Leinonen H, Levonen A-L. The Keap1-Nrf2 pathway: Mechanisms of activation and dysregulation in cancer. Redox Biology. 2013;1(1):45-9.

93.     Komatsu M, Kurokawa H, Waguri S, Taguchi K, Kobayashi A, Ichimura Y, et al. The selective autophagy substrate p62 activates the stress responsive transcription factor Nrf2 through inactivation of Keap1. Nat Cell Biol. 2010;12(3):213-23.

94.    Mathew R, Karp CM, Beaudoin B, Vuong N, Chen G, Chen HY, et al. Autophagy suppresses tumorigenesis through elimination of p62. Cell. 2009;137(6):1062-75.

95.    Duran A, Linares JF, Galvez AS, Wikenheiser K, Flores JM, Diaz-Meco MT, et al. The signaling adaptor p62 is an important NF-kappaB mediator in tumorigenesis. Cancer cell. 2008;13(4):343-54.

96.    Zhang H, Bosch-Marce M, Shimoda LA, Tan YS, Baek JH, Wesley JB, et al. Mitochondrial autophagy is an HIF-1-dependent adaptive metabolic response to hypoxia. J Biol Chem. 2008;283(16):10892-903.

97.    Hubbi ME, Hu H, Kshitiz, Ahmed I, Levchenko A, Semenza GL. Chaperone-mediated autophagy targets hypoxia-inducible factor-1alpha (HIF-1alpha) for lysosomal degradation. J Biol Chem. 2013;288(15):10703-14.

98.    Chen JL, Lin HH, Kim KJ, Lin A, Forman HJ, Ann DK. Novel roles for protein kinase Cdelta-dependent signaling pathways in acute hypoxic stress-induced autophagy. J Biol Chem. 2008;283(49):34432-44.

99.    Liu L, Feng D, Chen G, Chen M, Zheng Q, Song P, et al. Mitochondrial outer-membrane protein FUNDC1 mediates hypoxia-induced mitophagy in mammalian cells. Nat Cell Biol. 2012;14(2):177-85.

100.    Lazova R, Camp RL, Klump V, Siddiqui SF, Amaravadi RK, Pawelek JM. Punctate LC3B Expression Is a Common Feature of Solid Tumors and Associated with Proliferation, Metastasis, and Poor Outcome. Clinical Cancer Research. 2012;18(2):370-9.

101.    Zhao H, Yang M, Zhao J, Wang J, Zhang Y, Zhang Q. High expression of LC3B is associated with progression and poor outcome in triple-negative breast cancer. Medical Oncology. 2013;30(1):475.

102.    Fung C, Lock R, Gao S, Salas E, Debnath J. Induction of Autophagy during Extracellular Matrix Detachment Promotes Cell Survival. Molecular biology of the cell. 2008;19(3):797-806.

103.    Sandilands E, Serrels B, McEwan DG, Morton JP, Macagno JP, McLeod K, et al. Autophagic targeting of Src promotes cancer cell survival following reduced FAK signalling. Nat Cell Biol. 2012;14(1):51-60.

104.    Abbi S, Ueda H, Zheng C, Cooper LA, Zhao J, Christopher R, et al. Regulation of Focal Adhesion Kinase by a Novel Protein Inhibitor FIP200. Molecular biology of the cell. 2002;13(9):3178-91.

105.    Liang XH, Kleeman LK, Jiang HH, Gordon G, Goldman JE, Berry G, et al. Protection against Fatal Sindbis Virus Encephalitis by Beclin, a Novel Bcl-2-Interacting Protein. Journal of Virology. 1998;72(11):8586-96.

106.    Shen S, Kepp O, Michaud M, Martins I, Minoux H, Metivier D, et al. Association and dissociation of autophagy, apoptosis and necrosis by systematic chemical study. Oncogene. 2011;30(45):4544-56.

107.    Paglin S, Lee NY, Nakar C, Fitzgerald M, Plotkin J, Deuel B, et al. Rapamycin-sensitive pathway regulates mitochondrial membrane potential, autophagy, and survival in irradiated MCF-7 cells. Cancer research. 2005;65(23):11061-70.

108.    Kim KW, Moretti L, Mitchell LR, Jung DK, Lu B. Endoplasmic Reticulum Stress Mediates Radiation-Induced Autophagy via PERK-eIF2α in Caspase-3/7 Deficient Cells. Oncogene. 2010;29(22):3241-51.

109.    Avivar-Valderas A, Salas E, Bobrovnikova-Marjon E, Diehl JA, Nagi C, Debnath J, et al. PERK integrates autophagy and oxidative stress responses to promote survival during extracellular matrix detachment. Molecular and cellular biology. 2011;31(17):3616-29.

110.    Qadir MA, Kwok B, Dragowska WH, To KH, Le D, Bally MB, et al. Macroautophagy inhibition sensitizes tamoxifen-resistant breast cancer cells and enhances mitochondrial depolarization. Breast cancer research and treatment. 2008;112(3):389-403.

111. Samaddar JS, Gaddy VT, Duplantier J, Thandavan SP, Shah M, Smith MJ, et al. A role for macroautophagy in protection against 4-hydroxytamoxifen-induced cell death and the development of antiestrogen resistance. Molecular cancer therapeutics. 2008;7(9):2977-87.

112. Cook KL, Shajahan AN, Wärri A, Jin L, Hilakivi-Clarke LA, Clarke R. Glucose-Regulated Protein 78 Controls Cross-talk between Apoptosis and Autophagy to Determine Antiestrogen Responsiveness. Cancer research. 2012;72(13):3337-49.

113. Gonzalez-Malerva L, Park J, Zou L, Hu Y, Moradpour Z, Pearlberg J, et al. High-throughput ectopic expression screen for tamoxifen resistance identifies an atypical kinase that blocks autophagy. Proceedings of the National Academy of Sciences of the United States of America. 2011;108(5):2058-63.

114. Oltersdorf T, Elmore SW, Shoemaker AR, Armstrong RC, Augeri DJ, Belli BA, et al. An inhibitor of Bcl-2 family proteins induces regression of solid tumours. Nature. 2005;435(7042):677-81.

115. Pattingre S, Tassa A, Qu X, Garuti R, Liang XH, Mizushima N, et al. Bcl-2 antiapoptotic proteins inhibit Beclin 1-dependent autophagy. Cell. 2005;122(6):927-39.

116. Maiuri MC, Le Toumelin G, Criollo A, Rain JC, Gautier F, Juin P, et al. Functional and physical interaction between Bcl-X(L) and a BH3-like domain in Beclin-1. Embo j. 2007;26(10):2527-39.

117. Manic G, Obrist F, Kroemer G, Vitale I, Galluzzi L. Chloroquine and hydroxychloroquine for cancer therapy. Molecular & Cellular Oncology. 2014;1(1):e29911.

118. Settembre C, Zoncu R, Medina DL, Vetrini F, Erdin S, Erdin S, et al. A lysosome-to-nucleus signalling mechanism senses and regulates the lysosome via mTOR and TFEB. The EMBO Journal. 2012;31(5):1095-108.

119. Kaini RR, Sillerud LO, Zhaorigetu S, Hu C-AA. Autophagy Regulates Lipolysis and Cell Survival Through Lipid Droplet Degradation in Androgen Sensitive Prostate Cancer Cells. The Prostate. 2012;72(13):1412-22.

120. Jiang Q, Yeh S, Wang X, Xu D, Zhang Q, Wen X, et al. Targeting androgen receptor leads to suppression of prostate cancer via induction of autophagy. The Journal of urology. 2012;188(4):1361-8.

121. Li M, Jiang X, Liu D, Na Y, Gao GF, Xi Z. Autophagy protects LNCaP cells under androgen deprivation conditions. Autophagy. 2008;4(1):54-60.

122. Bennett HL, Stockley J, Fleming JT, Mandal R, O'Prey J, Ryan KM, et al. Does androgen-ablation therapy (AAT) associated autophagy have a pro-survival effect in LNCaP human prostate cancer cells? BJU international. 2013;111(4):672-82.

123. Nguyen HG, Yang JC, Kung HJ, Shi XB, Tilki D, Lara PN, Jr., et al. Targeting autophagy overcomes Enzalutamide resistance in castration-resistant prostate cancer cells and improves therapeutic response in a xenograft model. Oncogene. 2014;33(36):4521-30.

124. Bennett HL, Fleming JT, O'Prey J, Ryan KM, Leung HY. Androgens modulate autophagy and cell death via regulation of the endoplasmic reticulum chaperone glucose-regulated protein 78/BiP in prostate cancer cells. Cell death & disease. 2010;1:e72.

125. Shi Y, Han JJ, Tennakoon JB, Mehta FF, Merchant FA, Burns AR, et al. Androgens Promote Prostate Cancer Cell Growth through Induction of Autophagy. Molecular Endocrinology. 2013;27(2):280-95.

126. Blessing AM, Rajapakshe K, Reddy Bollu L, Shi Y, White MA, Pham AH, et al. Transcriptional regulation of core autophagy and lysosomal genes by the androgen receptor promotes prostate cancer progression. Autophagy. 2017;13(3):506-21.

127. Giampietri C, Petrungaro S, Padula F, D'Alessio A, Marini ES, Facchiano A, et al. Autophagy modulators sensitize prostate epithelial cancer cell lines to TNF-alpha-dependent apoptosis. Apoptosis. 2012;17(11):1210-22.

128. Evans JM, Donnelly LA, Emslie-Smith AM, Alessi DR, Morris AD. Metformin and reduced risk of cancer in diabetic patients. BMJ (Clinical research ed). 2005;330(7503):1304-5.

129. Colquhoun AJ, Venier NA, Vandersluis AD, Besla R, Sugar LM, Kiss A, et al. Metformin enhances the antiproliferative and apoptotic effect of bicalutamide in prostate cancer. Prostate cancer and prostatic diseases. 2012;15(4):346-52.

130. Ouyang D-Y, Xu L-H, He X-H, Zhang Y-T, Zeng L-H, Cai J-Y, et al. Autophagy is differentially induced in prostate cancer LNCaP, DU145 and PC-3 cells via distinct splicing profiles of ATG5. Autophagy. 2013;9(1):20-32.

131. Ohgami RS, Campagna DR, McDonald A, Fleming MD. The Steap proteins are metalloreductases. Blood. 2006;108(4):1388-94.

132. Gomes IM, Maia CJ, Santos CR. STEAP proteins: from structure to applications in cancer therapy. Molecular cancer research : MCR. 2012;10(5):573-87.

133. Warkentin E, Mamat B, Sordel-Klippert M, Wicke M, Thauer RK, Iwata M, et al. Structures of F(420)H(2):NADP(+) oxidoreductase with and without its substrates bound. The EMBO Journal. 2001;20(23):6561-9.

134. Ohgami RS, Campagna DR, Greer EL, Antiochos B, McDonald A, Chen J, et al. Identification of a ferrireductase required for efficient transferrin-dependent iron uptake in erythroid cells. Nature genetics. 2005;37(11):1264-9.

135. Ohgami RS, Campagna DR, McDonald A, Fleming MD. The Steap proteins are metalloreductases. Blood. 2006;108(4):1388-94.

136. Zhang F, Tao Y, Zhang Z, Guo X, An P, Shen Y, et al. Metalloreductase Steap3 coordinates the regulation of iron homeostasis and inflammatory responses. Haematologica. 2012;97(12):1826-35.

137. Gauss GH, Kleven MD, Sendamarai AK, Fleming MD, Lawrence CM. The Crystal Structure of Six-transmembrane Epithelial Antigen of the Prostate 4 (Steap4), a Ferri/Cuprireductase, Suggests a Novel Interdomain Flavin-binding Site. The Journal of Biological Chemistry. 2013;288(28):20668-82.

138. Kleven MD, Dlakic M, Lawrence CM. Characterization of a single b-type heme, FAD, and metal binding sites in the transmembrane domain of six-transmembrane epithelial antigen of the prostate (STEAP) family proteins. J Biol Chem. 2015;290(37):22558-69.

139. Zhou J, Ye S, Fujiwara T, Manolagas SC, Zhao H. Steap4 plays a critical role in osteoclastogenesis in vitro by regulating cellular iron/reactive oxygen species (ROS) levels and cAMP response element-binding protein (CREB) activation. J Biol Chem. 2013;288(42):30064-74.

140. Korkmaz KS, Elbi C, Korkmaz CG, Loda M, Hager GL, Saatcioglu F. Molecular cloning and characterization of STAMP1, a highly prostate-specific six transmembrane protein that is overexpressed in prostate cancer. J Biol Chem. 2002;277(39):36689-96.

141. Korkmaz CG, Korkmaz KS, Kurys P, Elbi C, Wang L, Klokk TI, et al. Molecular cloning and characterization of STAMP2, an androgen-regulated six transmembrane protein that is overexpressed in prostate cancer. Oncogene. 2005;24(31):4934-45.

142. Bonifacino JS, Dell'Angelica EC. Molecular Bases for the Recognition of Tyrosine-based Sorting Signals. The Journal of Cell Biology. 1999;145(5):923-6.

143. Porkka KP, Helenius MA, Visakorpi T. Cloning and characterization of a novel six-transmembrane protein STEAP2, expressed in normal and malignant prostate. Laboratory investigation; a journal of technical methods and pathology. 2002;82(11):1573-82.

144. Wang L, Jin Y, Arnoldussen YJ, Jonson I, Qu S, Maelandsmo GM, et al. STAMP1 is both a proliferative and an antiapoptotic factor in prostate cancer. Cancer research. 2010;70(14):5818-28.

145. Sikkeland J, Saatcioglu F. Differential Expression and Function of Stamp Family Proteins in Adipocyte Differentiation. PLOS ONE. 2013;8(7):e68249.

146. Gonen-Korkmaz C, Sevin G, Gokce G, Arun MZ, Yildirim G, Reel B, et al. Analysis of tumor necrosis factor alpha-induced and nuclear factor kappaB-silenced LNCaP prostate cancer cells by RT-qPCR. Experimental and therapeutic medicine. 2014;8(6):1695-700.

147. Arner P, Stenson BM, Dungner E, Naslund E, Hoffstedt J, Ryden M, et al. Expression of six transmembrane protein of prostate 2 in human adipose tissue associates with adiposity and insulin resistance. The Journal of clinical endocrinology and metabolism. 2008;93(6):2249-54.

148. Wellen KE, Fucho R, Gregor MF, Furuhashi M, Morgan C, Lindstad T, et al. Coordinated regulation of nutrient and inflammatory responses by STAMP2 is essential for metabolic homeostasis. Cell. 2007;129(3):537-48.

149. Jin Y, Wang L, Qu S, Sheng X, Kristian A, Maelandsmo GM, et al. STAMP2 increases oxidative stress and is critical for prostate cancer. EMBO molecular medicine. 2015;7(3):315-31.

150. Moreno-Navarrete JM, Ortega F, Serrano M, Perez-Perez R, Sabater M, Ricart W, et al. Decreased STAMP2 expression in association with visceral adipose tissue dysfunction. The Journal of clinical endocrinology and metabolism. 2011;96(11):E1816-25.

151. Ramadoss P, Chiappini F, Bilban M, Hollenberg AN. Regulation of hepatic six transmembrane epithelial antigen of prostate 4 (STEAP4) expression by STAT3 and CCAAT/enhancer-binding protein alpha. J Biol Chem. 2010;285(22):16453-66.

152. Kim HY, Park SY, Lee MH, Rho JH, Oh YJ, Jung HU, et al. Hepatic STAMP2 alleviates high fat diet-induced hepatic steatosis and insulin resistance. Journal of Hepatology. 2015;63(2):477-85.

153. Moldes M, Lasnier F, Gauthereau X, Klein C, Pairault J, Feve B, et al. Tumor necrosis factor-alpha-induced adipose-related protein (TIARP), a cell-surface protein that is highly induced by tumor necrosis factor-alpha and adipose conversion. J Biol Chem. 2001;276(36):33938-46.

154. Zhang CM, Chi X, Wang B, Zhang M, Ni YH, Chen RH, et al. Downregulation of STEAP4, a highly-expressed TNF-alpha-inducible gene in adipose tissue, is associated with obesity in humans. Acta pharmacologica Sinica. 2008;29(5):587-92.

155. Chen X, Zhu C, Ji C, Zhao Y, Zhang C, Chen F, et al. STEAP4, a gene associated with insulin sensitivity, is regulated by several adipokines in human adipocytes. International journal of molecular medicine. 2010;25(3):361-7.

156. Fasshauer M, Kralisch S, Klier M, Lossner U, Bluher M, Chambaut-Guerin AM, et al. Interleukin-6 is a positive regulator of tumor necrosis factor alpha-induced adipose-related protein in 3T3-L1 adipocytes. FEBS letters. 2004;560(1-3):153-7.

157. Kralisch S, Sommer G, Weise S, Lipfert J, Lossner U, Kamprad M, et al. Interleukin-1beta is a positive regulator of TIARP/STAMP2 gene and protein expression in adipocytes in vitro. FEBS letters. 2009;583(7):1196-200.

158. Wu L, Chen X, Zhao J, Martin B, Zepp JA, Ko JS, et al. A novel IL-17 signaling pathway controlling keratinocyte proliferation and tumorigenesis via the TRAF4-ERK5 axis. J Exp Med. 2015;212(10):1571-87.

159. ten Freyhaus H, Calay ES, Yalcin A, Vallerie SN, Yang L, Calay ZZ, et al. Stamp2 controls macrophage inflammation through nicotinamide adenine dinucleotide phosphate homeostasis and protects against atherosclerosis. Cell metabolism. 2012;16(1):81-9.

160. Wang SB, Lei T, Zhou LL, Zheng HL, Zeng CP, Liu N, et al. Functional analysis and transcriptional regulation of porcine six transmembrane epithelial antigen of prostate 4 (STEAP4) gene and its novel variant in hepatocytes. The International Journal of Biochemistry & Cell Biology. 2013;45(3):612-20.

161. Isobe T, Baba E, Arita S, Komoda M, Tamura S, Shirakawa T, et al. Human STEAP3 maintains tumor growth under hypoferric condition. Exp Cell Res. 2011;317(18):2582-91.

162. Lambe T, Simpson RJ, Dawson S, Bouriez-Jones T, Crockford TL, Lepherd M, et al. Identification of a Steap3 endosomal targeting motif essential for normal iron metabolism. Blood. 2009;113(8):1805-8.

163. McCarthy RC, Kosman DJ. Mechanistic analysis of iron accumulation by endothelial cells of the BBB. Biometals : an international journal on the role of metal ions in biology, biochemistry, and medicine. 2012;25(4):665-75.

164. Zhang X, Steiner MS, Rinaldy A, Lu Y. Apoptosis induction in prostate cancer cells by a novel gene product, pHyde, involves caspase-3. Oncogene. 2001;20(42):5982-90.

165. Passer BJ, Nancy-Portebois V, Amzallag N, Prieur S, Cans C, Roborel de Climens A, et al. The p53-inducible TSAP6 gene product regulates apoptosis and the cell cycle and interacts with Nix and the Myt1 kinase. Proceedings of the National Academy of Sciences of the United States of America. 2003;100(5):2284-9.

166. Yu X, Harris SL, Levine AJ. The Regulation of Exosome Secretion: a Novel Function of the p53 Protein. Cancer research. 2006;66(9):4795-801.

167. Nielsen OH, Bjerrum JT, Csillag C, Nielsen FC, Olsen J. Influence of Smoking on Colonic Gene Expression Profile in Crohn's Disease. PLOS ONE. 2009;4(7):e6210.

168. Cheng R, Qiu J, Zhou XY, Chen XH, Zhu C, Qin DN, et al. Knockdown of STEAP4 inhibits insulin-stimulated glucose transport and GLUT4 translocation via attenuated phosphorylation of Akt, independent of the effects of EEA1. Molecular medicine reports. 2011;4(3):519-23.

169. Tamura T, Chiba J. STEAP4 regulates focal adhesion kinase activation and CpG motifs within STEAP4 promoter region are frequently methylated in DU145, human androgen-independent prostate cancer cells. International journal of molecular medicine. 2009;24(5):599-604.

170. Lindstad T, Qu S, Sikkeland J, Jin Y, Kristian A, Maelandsmo GM, et al. STAMP2 is required for human adipose-derived stem cell differentiation and adipocyte-facilitated prostate cancer growth in vivo. Oncotarget. 2016.

171. Abeshouse A, Ahn J, Akbani R, Ally A, Amin S, Andry Christopher D, et al. The Molecular Taxonomy of Primary Prostate Cancer. Cell.163(4):1011-25.

172. Kabeya Y, Mizushima N, Ueno T, Yamamoto A, Kirisako T, Noda T, et al. LC3, a mammalian homologue of yeast Apg8p, is localized in autophagosome membranes after processing. The EMBO Journal. 2000;19(21):5720-8.

173. Klionsky DJ, Abdelmohsen K, Abe A, Abedin MJ, Abeliovich H, Acevedo Arozena A, et al. Guidelines for the use and interpretation of assays for monitoring autophagy (3rd edition). Autophagy. 2016;12(1):1-222.

174. Hurley JH, Young LN. Mechanisms of Autophagy Initiation. Annu Rev Biochem. 2017.

175. Datan E, Shirazian A, Benjamin S, Matassov D, Tinari A, Malorni W, et al. mTOR/p70S6K signaling distinguishes routine, maintenance-level autophagy from autophagic cell death during influenza A infection. Virology. 2014;452–453:175-90.

176. Fullgrabe J, Ghislat G, Cho DH, Rubinsztein DC. Transcriptional regulation of mammalian autophagy at a glance. Journal of cell science. 2016;129(16):3059-66.

177. Zoncu R, Bar-Peled L, Efeyan A, Wang S, Sancak Y, Sabatini DM. mTORC1 senses lysosomal amino acids through an inside-out mechanism that requires the vacuolar H(+)-ATPase. Science (New York, NY). 2011;334(6056):678-83.

178. Kimura S, Noda T, Yoshimori T. Dissection of the autophagosome maturation process by a novel reporter protein, tandem fluorescent-tagged LC3. Autophagy. 2007;3(5):452-60.

179. Mauvezin C, Neufeld TP. Bafilomycin A1 disrupts autophagic flux by inhibiting both V-ATPase-dependent acidification and Ca-P60A/SERCA-dependent autophagosome-lysosome fusion. Autophagy. 2015;11(8):1437-8.

180. Wu YT, Tan HL, Shui G, Bauvy C, Huang Q, Wenk MR, et al. Dual role of 3-methyladenine in modulation of autophagy via different temporal patterns of inhibition on class I and III phosphoinositide 3-kinase. J Biol Chem. 2010;285(14):10850-61.

181. White E. The role for autophagy in cancer. The Journal of Clinical Investigation. 2015;125(1):42-6.

182. Allen GFG, Toth R, James J, Ganley IG. Loss of iron triggers PINK1/Parkin-independent mitophagy. EMBO reports. 2013;14(12):1127-35.

183. Qin DN, Zhu JG, Ji CB, Chunmei S, Kou CZ, Zhu GZ, et al. Monoclonal antibody to six transmembrane epithelial antigen of prostate-4 influences insulin sensitivity by attenuating phosphorylation of P13K (P85) and Akt: possible mitochondrial mechanism. Journal of bioenergetics and biomembranes. 2011;43(3):247-55.

184. Qin DN, Kou CZ, Ni YH, Zhang CM, Zhu JG, Zhu C, et al. Monoclonal antibody to the six-transmembrane epithelial antigen of prostate 4 promotes apoptosis and inhibits proliferation and glucose uptake in human adipocytes. International journal of molecular medicine. 2010;26(6):803-11.

185. Filomeni G, De Zio D, Cecconi F. Oxidative stress and autophagy: the clash between damage and metabolic needs. Cell Death Differ. 2015;22(3):377-88.

186. Wu Y, Li X, Xie W, Jankovic J, Le W, Pan T. Neuroprotection of deferoxamine on rotenone-induced injury via accumulation of HIF-1 alpha and induction of autophagy in SH-SY5Y cells. Neurochemistry international. 2010;57(3):198-205.

187. Boutin B, Tajeddine N, Vandersmissen P, Zanou N, Van Schoor M, Mondin L, et al. Androgen deprivation and androgen receptor competition by bicalutamide induce autophagy of hormone-resistant prostate cancer cells and confer resistance to apoptosis. The Prostate. 2013;73(10):1090-102.

# 7 Paper I

# Paper I

Working title:

# The role of STAMP2 in the regulation of autophagy in prostate cancer cells.

Matthew Ng[1], Yang Jin[1], Anne Simonsen[2,3], Fahri Saatcioglu[1,4]

[1]Department of Biosciences, University of Oslo, Norway

[2]Department of Basic Medical Sciences, University of Oslo, Norway

To whom correspondence should be addressed:

[3]anne.simonsen@medisin.uio.no and [4]fahri.saatcioglu@ibv.uio.no

# Abstract

Autophagy is a process of catabolic degradation of cellular components in the lysosomes. In prostate cancer (PCa), autophagy has gained increased attention following findings that it contributes to tumor growth, survival and treatment resistance. Here, we investigated the potential role of Six Transmembrane of Prostate 2 (STAMP2), a driver of PCa progression, in the regulation of autophagy in PCa cells. We show that STAMP2 (also known as Six transmembrane epithelial antigen of prostate 4, STEAP4) inhibits LC3 lipidation and puncta formation, as well as the degradation of long-lived proteins. siRNA mediated knockdown of STAMP2 led to upregulation of a number of autophagy genes, such as *p62* (also known as *SQSTM1)* encoding sequestosome 1 and *MAP1LC3b* encoding Microtubule-associate proteins 1A/1B light chain 3B (LC3b). This was corroborated by gene expression data available on primary PCa, which shows that STAMP2 levels are inversely correlated with LC3 family gene expression. Furthermore, STAMP2 knockdown increased Unc-51 Like Autophagy Activating Kinase 1 (ULK1) activation, suggesting regulation at the early stages of autophagy. Consistently, STAMP2 knockdown increased Transcription Factor EB (TFEB) target gene while TFEB was predominantly nuclear indicating its activation. Additionally, the amount of lysosome structures was higher in STAMP2 depleted cells. These data suggest that STAMP2 is involved in repression of the autophagic pathway through regulation of transcriptional events and post-translational modifications. Further studies are required to provide a mechanistic framework for these observations.

# Introduction

Macroautophagy (henceforth autophagy), is a catabolic process whereby cytosolic components are engulfed in double bilayered membranes called autophagosomes. As the autophagosomes mature, they undergo fusion with lysosomes such that their contents are degraded by the hydrolases contained within the lysosomal lumen (1). Autophagy is a homeostatic process that is central in both normal and cancer cell biology. Autophagy can work against cancer development during the early stages of carcinogenesis; however, in developed tumors it is considered to play a pro-survival role (2). Defects in autophagy leads to accumulation of damaged organelles, aberrant intracellular signaling, increases in cellular reactive oxygen species (ROS) and DNA damage (3, 4) which can drive both normal and cancer cells into death. Conversely, autophagy is induced during cancer treatment and it facilitates treatment resistance in multiple cancer types such as cancers of the breast (5, 6), lung (7, 8), liver (9), and prostate (10-13).

Worldwide, prostate cancer (PCa) is the second most commonly diagnosed cancer in men, second only to lung cancer (14). PCa cells are often reliant on androgens to maintain growth and survival. This dependence of PCa cells on androgens provides an additional avenue to target PCa. Repressing the AR signaling pathway using androgen deprivation therapies usually results in regression of the tumor, which unfortunately often relapses at a later stage in an androgen ablation insensitive form called castration resistant prostate cancer (CRPC) (15). Direct targeting of the AR by antagonists such as bicalutamide and enzalutamide, or the removal of androgens from *in vitro* cell culture models leads to increased autophagic flux that contributes to PCa cell survival (11, 13). Inhibition of autophagy in combination with ADT led to synergistic inhibition of tumor cell growth *in vitro* (11, 16) as well as *in vivo* (17). These findings have spurred multiple clinical trials in PCa patients where autophagy is modulated in combination with other canonical therapies.

The STAMP2 is a membrane protein that is embedded through its six transmembrane domains (18). It contains an oxidoreductase domain on its disordered N-terminal tail that is necessary for its physiological functions in adipose (19), osteoclast (20) and prostate tissues (21). STAMP2 is localized to transferrin receptor positive early endosomal compartments and is suspected to be involved in regulating endocytic and secretory pathways. STAMP2 is an androgen-regulated gene that is crucial for PCa cell growth and progression (18). The ferrireductase domain in the N-terminal region of STAMP2 is indispensable for driving PCa

growth, at least in part, through the generation of ROS (21). Here we show that depletion of STAMP2 induces autophagy in PCa cells and that the effect is mediated, in part, through ULK activation and TFEB regulated autophagy gene expression.

# Methods and materials

### Cell culture

LNCaP (ATCC# CRL-1740) and VCaP (ATCC#CRL-2876) cells were obtained from American Type Culture Collection (ATCC) and was maintained in RPMI40 and DMEM (Lonza; 10% Fetal Bovine Serum, 5 mg/ml penicillin/streptomycin, 200mM $L$-Glutamine) respectively at $37^{o}$C with 5% $CO_2$ in a humidified sterilized incubator. The cells are routinely split at 90% confluency and the medium changed every 3 days. All cells were confirmed to be mycoplasma free using the MycoAlert Mycoplasma Detection Kit (Lonza). Cells stably expressing shRNAs were maintained in growth media containing 0.2 µg/ml puromycin. For starvation treatments, the cells are washed in PBS and incubated in EBSS (Gibco). Autophagy is inhibited by treatment with 100 nM Bafilomycin A1 (BafA1; Enzo) for the indicated times.

### siRNA transfection

Gene knockdown was performed using Lipofectamine RNAiMax (Invitrogen) according to manufacturer's protocol for reverse transfection. Reverse transfection was performed according to manufacturer's instructions. Cells were incubated in antibiotic free media containing a final siRNA concentration of 10nM for a minimum of 48 hours. siRNA oligonucleotides were STAMP2-In3 AATGCAGAGTACCTTGCTCAT.

### Western Blot Analysis

Western blotting was performed according to standard protocols. After separation by SDS-PAGE, the proteins in the polyacrylamide gel were transferred to methanol activated polyvinylidene fluoride (PVDF) membranes by a standard semi dry transfer method. The membranes were thereafter blocked in 5% non-fat milk dissolved in tris-buffered saline with 0.1% Tween-20 (TBS-T). The membranes are then incubated overnight in primary antibody diluted in TBS-T. The following primary antibodies were used: rabbit anti-ULK1 (Santa Cruz, Sc-33192, 1:1000), rabbit anti-LC3 (MBL, PM036, 1:1000), rabbit anti-phospho-ULK1 Ser555 (Cell signaling, 5869S, 1:1000), rabbit anti-phospho-ULK1 Ser757 (Cell signaling, 6888S,

1:1000), mouse anti-ACTB (Sigma Aldrich, 1:1000), mouse anti-GAPDH (Santa Cruz, 1:1000), rabbit anti-HDAC1 (Proteintech, 1:1000), rabbit anti-TFEB (Cell Signaling, 4240S, 1:1000), mouse anti-p62 (BD biosciences, 1:1000), rabbit anti-phospho-p70S6K Thr389 (Cell Signaling, 9205, 1:1000), rabbit anti-p70S6K (Cell Signaling, 9202, 1:1000), rabbit anti-phospho-AMPK Thr172 (Cell Signaling, 2531, 1:1000), rabbit anti-AMPK (Cell signaling, 2532, 1:1000). The blocked membranes were then incubated in secondary antibodies (HRP-conjugated anti-rabbit IgG antibody (1:10000 dilution) or HRP-conjugated anti-mouse IgG antibody (1:10000 dilution) in TBST for 1 hour at room temperature. Chemiluminescence was detected using the ECL Western Blotting System according to manufacturer's instructions.

**Long-lived protein degradation**

To label long-lived proteins, LNCaP cells were incubated in medium containing 10 mM $^{14}$C-L-Valine (Perkin Elmer) for 48 hours. Then the radioactive medium was removed and the cells were replenished in regular growth medium for 16 hours to allow for the degradation of short-lived proteins. The cells were washed and starved or not in the presence of 100 nM BafA1 or vehicle for 4 hours. The supernatant was then collected and trichloroacetic acid (Sigma Aldrich) was added to precipitate non-degraded radioactive proteins. The supernatant and pellet fraction was dissolved in UltimaGold liquid scintillation cocktail (Perkin Elmer). The amount of radioactivity was counted at 3 minutes per sample in a liquid scintillation counter (Tri-Carb 3100TR, Perkin Elmer). Protein degradation was described as the ratio of non-degraded long-lived proteins relative to total detected radioactivity.

**Synthesis of cDNA and RT-qPCR**

Total RNA was isolated using the TRIzol Reagent (Sigma Aldrich) as described by the manufacturer's instructions. The RNA pellet is washed in 70% EtOH and resolved in nuclease free water. RNA purity and concentration were determined using NanoDrop 1000 (ThermoScientific, Nanodrop technology). The RNA was reversed transcribed to synthesize complementary DNA (cDNA) using SuperScript II Reverse Transcriptase (Invitrogen) according to the protocol provided by the manufacturer. The relative expression level was normalized against selected housekeeping genes, glyceraldehyde-3-phosphate dehydrogenase (*GAPDH*) or TATA-binding protein (*TBP*). Primer sequences were as follows;

*MAP1LC3B* fwd. 5' CAGCTTCCTGTTCTGGATAAA 3' and rev. 5' TAATCTTCCGCGAA TGTCG 3'; *MAP1LC3A* fwd. 5' GTGAACCAGCACAGCAT 3' and rev. 5' AGATATACCA

GATGCGGAGG 3'; *ATG5* fwd. 5' AGCAACTCTGGATGGGATTG 3' and rev. 5' GTCTG
TTGCTGACTTTCTGGA 3'; *BECN1* fwd. 5' AAGAGGTTGAGAAAGGCGAG 3' and rev.
5' CGAGGATAAGGTAGTTTTGGGT 3'; *SQSTM1* fwd. 5' AATCAGCTTCTGGTCCATC
G 3' and rev. 5' CTCGTGCCTCCCTTTTCTT 3'; *STAMP2* fwd. 5' TTGGTAGCTCTGGGA
TTTG 3' and rev. 5' CCTCCACGATTTACCTAAGAG 3'; *GAPDH* fwd. 5' GTCAGTGGT
GGACCTGACCT 3' and rev. 5' AGGAGACTGAAGTTGTCGCT3'; *ACTB* fwd. 5' GGCTA
CAGCTTCACCACCAC 3' and rev. 5' TCTCGATGCTCGACGGACTG 3'; *TBP* fwd. 5' G
AGCTGTGATGTGAAGTTTCC 3' and rev. 5' ATGTCTTACTAGTTTGGGTCT 3'; *NPC1*
fwd. 5' GCCTACCGAGTATTTCCTTAC 3' and rev. 5' GATAGAAGTTGGAGCCACAC
3'; *MCOLN1* fwd. 5' TCTCCCAGCTCTACCTTTAC 3' and rev. 5' GATGCTGTGGTAGT
TCGTAG 3'; ATG5 fwd. 5' AGCAACTCTGGATGGGATTG 3' and rev. 5' GTCTGTTGCT
GACTTTCTGGA 3'.

## Immunofluorescence microscopy

Cells were grown in 24 well plates on sterilized glass coverslips and fixed in 4% PFA (pH 7.2)
for 15 min. After fixation, the cells were incubated in LC3 antibody (MBL; 1:100 dilution) for
1 hour, anti-rabbit alexafluor-488 antibody (Thermo Fisher Scientific; 1:400) for 45 minutes
and 0.3 µg/ml DAPI for 5 minutes at room temperature. The immune-labelled cells were then
fixed on glass slides with Mowiol and visualized on an automated Olympus ScanR microscope
equipped with a ULSAPO 40 X objective, and the results were quantified using the physiology
module available in the Zeiss Assaybuilder program. Lysosomes are labelled with the
LysoTracker Red DND-99 lysotrophic dye (Thermo Fisher Scientific). Lysotracker was added
into prewarmed growth media to achieve a final concentration of 50 nM for 30 minutes.

## Lentivirus transduction and stable cell line selection

HEK293T cells were transfected with lentivirus plasmids using the Trans-Lentiviral Packaging
Kit (Thermo Scientific) 64 hours post transfection, the media containing lentivirus was
collected and passed through a sterile filter. LNCaP cells to be transduced were then incubated
in the lentivirus containing media for 4 hours. The media was then removed and the cells were
incubated for 48 hours, and selected using 1µg/ml puromycin for 2 weeks. The cells were then
maintained in media containing 0.2µg/ml puromycin to maintain selection pressure.
Transduction efficiency was determined by qPCR. The shRNA targeting STAMP2

(TATCCATCACTCTTTGCTTGG) was expressed from a Lentiviral pLKO.1 vector (Open Biosystems, Thermo Fisher Scientific).

## Subcellular fractionation

Nuclear and cytoplasmic protein lysates were obtained using the Subcellular Protein Fractionation Kit for Cultured cells (Thermo Scientific) according to manufacturer's instructions.

## Bioinformatic analyses

RNA sequencing data from the cancer genome atlas study (TCGA) PCa cohort was used for correlation analysis of gene expression (22). The samples (N=499) were stratified two populations by the median based on STAMP2 expression. The differential expression of autophagy genes in two groups were presented in a boxplot.

## Microarray

LNCaP cells were treated with control or STAMP2 siRNA and incubated in growth media containing 10 nM R1881 (Sigma Aldrich) or an equal amount of 96% EtOH (Vehicle) for 48 hours before analysed by cDNA microarray analysis for gene expression profiling. RNA integrity was determined by a bioanalyser. Samples with RNA integrity number (RIN) greater than 7 were selected for downstream analysis. The RNA was amplified and hybridized to Illumina HumanHT-12 v4 arrays.

## Statistics

Significance was determined based on p-values derived from two-tailed, two-sample Student's t-test, and considered statistically significant only when $P \leq 0.05$.

# Results

**STAMP2 knockdown induces LC3 lipidation.**

Since the amount of phosphatidyl ethanolamine (PE) conjugated LC3 (LC3-II) is correlated to the amount of autophagosomes in a cell (23), the change of LC3-II in the presence and absence of the lysosomal inhibitor BafA1 was used as a readout of the autophagic flux. To investigate the potential effect of STAMP2 on autophagy, we estimated the amount of LC3-II in LNCaP cells upon siRNA-mediated STAMP2 knockdown. As shown in Fig. 1A, STAMP2 depletion increased the conversion of LC3-I into the LC3-II form by about two-fold compared to the control cells. In the consensus model of autophagy, the autophagosomes are concentrated with membrane bound LC3 and appear as puncta when immuno-labeled; thus, the number of LC3 puncta can be correlated to the amount of autophagosomes in the cell (Fig. 1C). We observed an increase in LC3 puncta when STAMP2 was depleted (Fig. 1B-C). The levels of LC3-I were also increased in STAMP2 knockdown cells (Fig. 1A), consistent with transcriptional upregulation of LC3b as shown in the gene expression data in the experiments presented below (Fig. 4C).

Changes in the autophagy adaptor protein p62 can also be used as a readout of autophagic flux (24). However, p62 levels did not accumulate upon BafA1 treatment, as might have been expected after the inhibition of lysosomal degradation (Fig. 1A), possibly due to protein precipitation during protein lysates preparations. p62 is accumulated upon BafA1 treatment in the experiment with STAMP2 overexpressing cells (Fig. 1D). In agreement with the inverse correlation between downregulated STAMP2 expression and increased autophagosome formation, ectopic STAMP2 expression in LNCaP cells decreased LC3 lipidation (Fig. 1D). The data suggest that STAMP2 may inhibit LC3 lipidation and autophagosome formation.
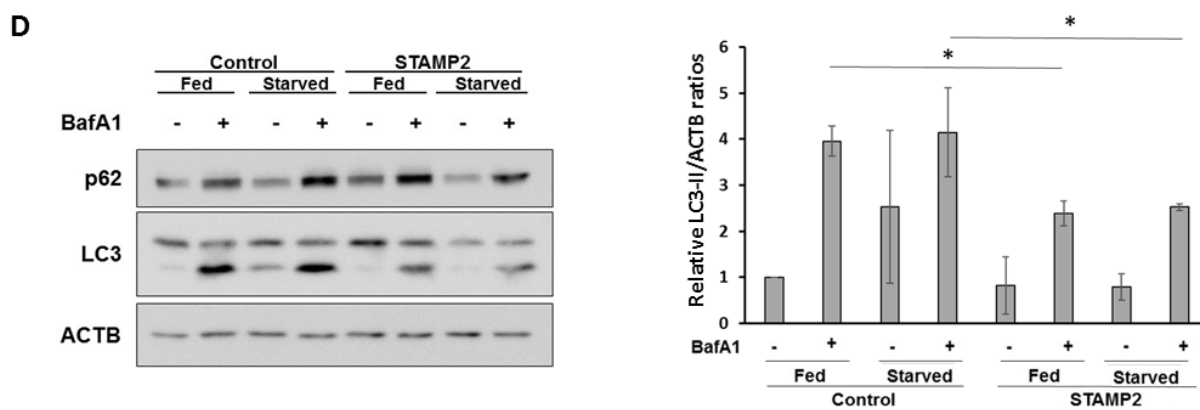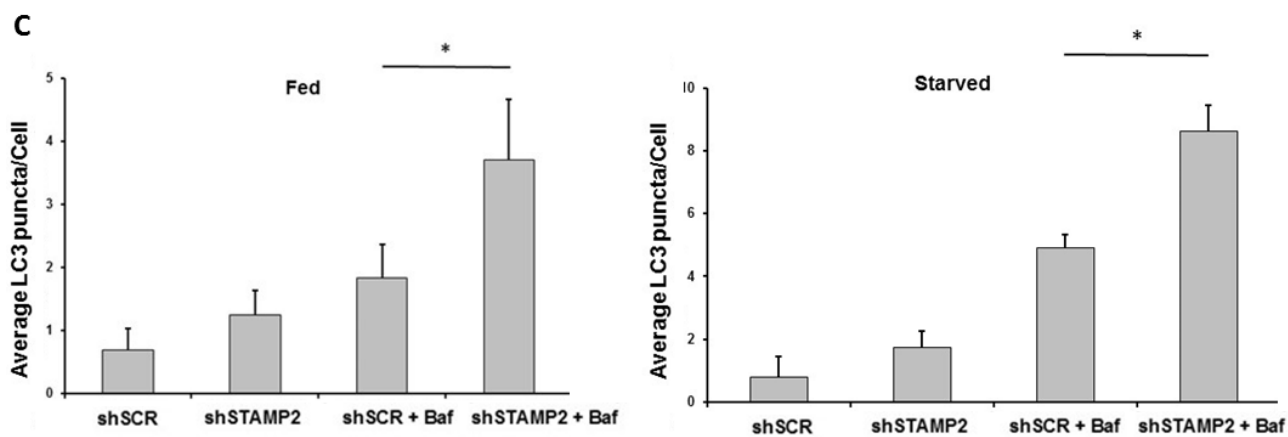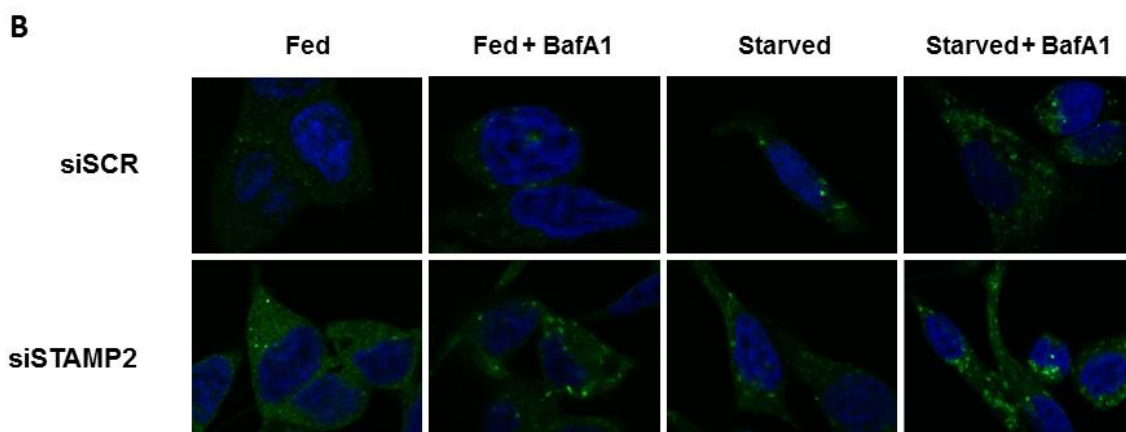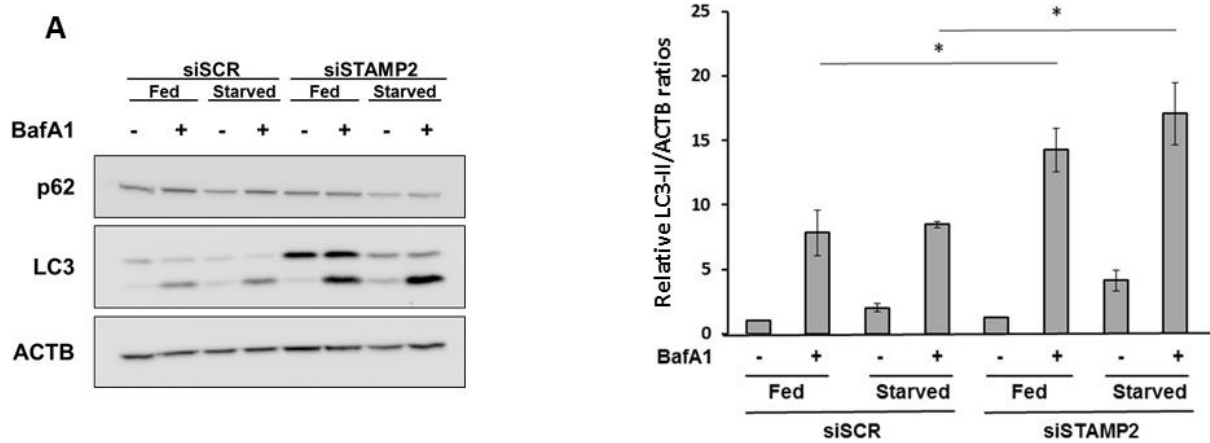
A



B

| | Fed | Fed + BafA1 | Starved | Starved + BafA1 |
|---|---|---|---|---|

siSCR

siSTAMP2

C



D

**Figure 1: LC3 lipidation and puncta formation was increased upon depletion of STAMP2.**

**A**. LNCaP cells were transiently transfected with control or STAMP2 siRNA. After 48 hours, the cells were either left fed or starved with EBSS for 4 hours in the presence of 100 nM BafA1 or vehicle. The protein levels of p62 and LC3 were determined by western blot analysis. Blots show the protein abundance of LC3 normalized to Beta-actin (ACTB). The bar graph (right panel) represents quantification of band intensities in of LC3 normalized to ACTB. The data presented are from three independent experiments **B**. Immunofluorescence microscopy analysis of LC3 puncta (green) in LNCaP cells treated as in A. Nuclei were stained by DAPI (blue). **C**. Quantification of LC3 puncta (green) of B. **D**. LNCaP cells stably expressing His-Tag (Control) or His-STAMP2 (STAMP2) is subjected to starvation and BafA1 treatment as in A. The cells were harvested and subjected to Western analysis of p62 and LC3 expression. The bar graph (right panel) represents quantification of band intensities in of LC3 normalized to ACTB. The data presented are from three independent experiments.

## STAMP2 depletion leads to increased lysosomal degradation.

Since the level of LC3 makes up only half of the LC3 family proteins in mammalian cells, it is not sufficient to fully represent and describe the autophagic flux. We therefore evaluated the degradation of autophagic substrates in the lysosomes. Long-lived proteins (LLPs) are preferentially degraded in lysosomes following autophagy. To determine the flux of LLP degradation, siRNA-treated LNCaP cells were incubated in growth media containing radioactive $^{14}$C-Valine to radioactively label LLPs. The cells were then chased with non-radioactive media. During the chase period, short-lived proteins are turned over in the cell and are resynthesized with non-radioactive valine, while radioactively labeled are not degraded and LLPs remain radioactively labelled in the cell. The degradation of LLP is calculated from the ratio of free radioactivity released into the supernatant (degraded LLP) against total radioactivity (supernatant + cells dissolved in KOH), and is displayed as the percentage of degraded LLP. The percentage of LLPs was obtained from the differences between Baf1 treated and untreated samples.

Upon STAMP2 knockdown, the degradation of radioactively labeled LLPs, in the form of free $^{14}$C-Valine, was increased in both fed and starved conditions (Fig. 2), indicating that degradation of cytoplasmic constituents through the lysosomes is increased when STAMP2 was lost, further confirming that STAMP2 represses autophagy.
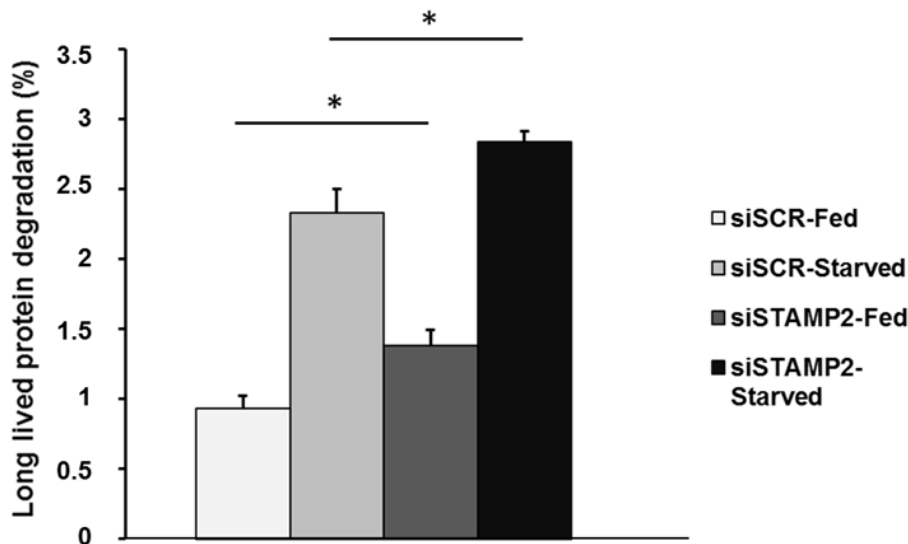
**Figure 2: Long-lived protein degradation is increased upon STAMP2 depletion.**

LNCaP cells were reverse transfected with control or STAMP2 siRNA. The cells were incubated in media containing ^{14}C-Valine for 48 hours, and in media containing non-radioactive valine for 16 hours. The cells were then either starved or not with EBSS in the presence or absence of BafA1 for 4 hours. Non-degraded LLPs are precipitated by TCA and sample radioactivity was analyzed on a liquid scintillation counter. The bar charts represent the relative ratios of acid-labile radioactivity versus total radioactivity in control and STAMP2 knockdown cells in both fed and starved conditions. The chart represents quantification of three independent experiments.

## STAMP2 is involved in ULK1 phosphorylation.

The main early regulators of autophagy are the nutrient sensors of the cell, mTOR and AMPK; each phosphorylating ULK1 on residues Serine 757 (S757) or Serine 555 (S555), respectively, to regulate downstream autophagy initiating events (25). We therefore assessed the phosphorylation of ULK1 to determine its activation. Starvation induces ULK1 phosphorylation at S555 by AMPK (25). We observed that in the fed state prior to starvation, ULK1 phosphorylation on S555 was increased upon STAMP2 knock down in LNCaP cells (Fig. 3A) as well as in VCaP cells (Fig. 3B). Interestingly, upon starvation, the phosphorylation of ULK1 at S555 was decreased in LNCaP in both control and STAMP2 knockdown cells, instead of increasing as would be expected given that AMPK is activated upon starvation. In VCaP cells this phosphorylation is decreased in STAMP2 knockdown cells but increased in cells treated with control siRNA. This difference indicates cell type specific responses towards starvation. The activation of mTORC1 was assessed by the phosphorylation of one of its substrates, p70S6K at Threonine 389. P-p70S6K was increased upon STAMP2 depletion prior
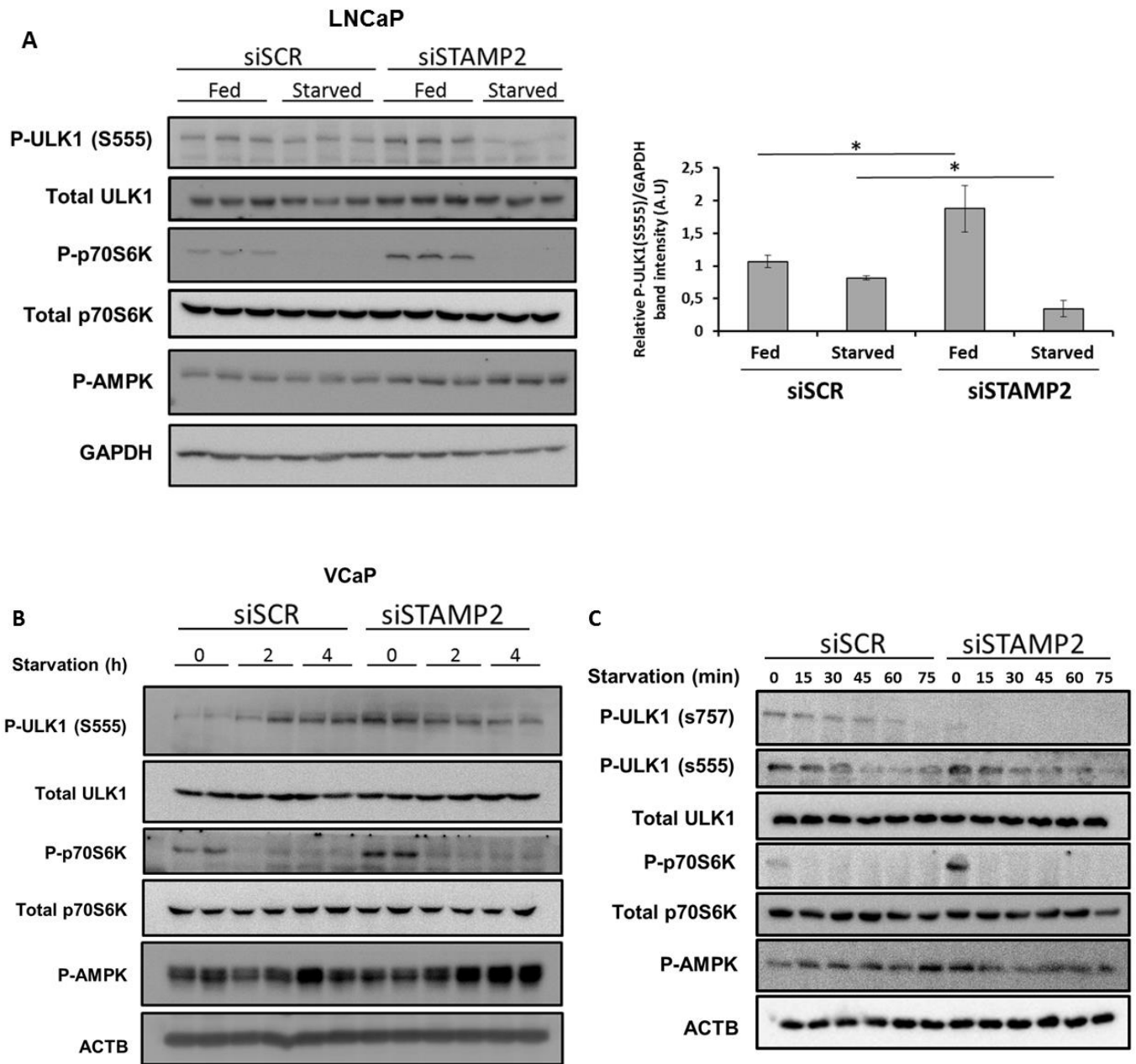
**Figure 3: Depletion of STAMP2 increases activating and decreases inhibitory phosphorylation on ULK1.**

**A** siRNA-treated LNCaP cells were starved or not for 1 hour in EBSS **B**. siRNA-treated VCaP cells were starved for the indicated times in EBSS. The cells were harvested and subjected to western analysis for protein expression of P-ULK1 (S555) and p70S6K. Total ULK1, total p70S6K and ACTB were used as loading control. **C**. siRNA treated LNCaP cells were starved for the indicated times in EBSS before subjected to western anaylsis of P-ULK1 (S757), P-ULK1 (S555), P-AMPK and P-p70S6K, Total ULK1, total p70S6K and ACTB were used as loading control.

to starvation in both LNCaP and VCaP cells, while it was abolished upon starvation. mTORC1 phosphorylates ULK1 on S757 to inhibit its association with Atg13 and FIP200. Irrelevant to mTORC1 activation, S757 phosphorylation of ULK1 was greatly decreased in LNCaP cells upon  STAMP2 knockdown (Fig. 3C). S757 phosphorylation of ULK1 was decreased during starvation, as expected, and was almost undetectable in STAMP2 knockdown cells. P-AMPK levels were unfortunately indiscernible due to lack of a suitable antibody. These results suggest that STAMP2 mediated regulation of autophagy in LNCaP cells involves the ULK complex and is independent of mTORC1 activity.

**Autophagy gene expression is modulated by STAMP2.**
As the LC3-I protein level was higher in STAMP2 knockdown cells even under fed conditions (Fig. 1A), we assessed whether *LC3* expression was regulated at the transcriptional level by employing real-time PCR (RT-qPCR) analysis. Gene expression of *MAP1LC3b* and *SQSTM1* were increased upon STAMP2 knockdown. However, the expression of other autophagy genes, such as *ATG5* and *BECN1*, were not affected (Fig. 4A). Conversely, reciprocal observations were reversed in cells stably overexpressing STAMP2 (Fig. 4B).

To assess if STAMP2 also affected LC3 gene expression in human PCa specimens as observed in the previous experiments (Fig. 2A-B), we analyzed the possible correlation between LC3 family and that of STAMP2 in a publicly available PCa RNA sequencing dataset of the TCGA PCa cohort (22). STAMP2 expression was separated into high and low expressing at the median and was stratified with that of *MAP1LC3A*, *MAP1LC3B*, *MAP1LC3C*, *GABARAP*, *GABARAPL1*, *GABARAPL2* and *SQSTM1*.  Gene expression for all members of the LC3 family, except *GABARPL1*, were found to be significantly inversely correlated (Fig. 4C). Consistent with the results from RT-qPCR in cell lines (Fig. 4A-B), *SQSTM1* expression in PCa was also higher in tumors with lower *STAMP2* expression.

**Figure 4: STAMP2 affects autophagy gene expression**

**A.** LNCaP cells stably transduced with control or STAMP2 shRNA lentiviral constructs were harvested, total RNA was isolated, reverse transcribed and subjected to RT-qPCR analysis (n = 3, p<0.05). **B.** Total RNA was collected from control and LNCaP cells stably expressing STAMP2 and gene expression was analysed by RT-qPCR. (n = 3, p<0.05) **C.** LC3 family (*GABARAP*, *-L1*, *-L2*, *MAP1LC3A*, *-B*, *-C*) and *p62* expression values were extracted from RNA sequencing data from Abeshouse et al (26). STAMP2 expression was stratified into high and low expression groups and autophagy gene expression were compared.

**TFEB target gene expression and nuclear translocation is increased upon STAMP2 depletion.**

TFEB is a master regulator of autophagy and directly regulates the expression of genes with known roles in lysosomal function (27). Global gene expression profiling by microarray analysis in siRNA treated LNCaP cells revealed that TFEB target gene expression was altered upon STAMP2 knockdown (Yang Jin et al., unpublished data). By analyzing the gene expression profile of STAMP2 knockdown LNCaP cells, we found that genes involved in lysosomal biogenesis and autophagy were upregulated (Fig. 5A). Inactive TFEB is sequestered in the cytoplasm by its interaction to 14-3-3 proteins. Upon activation, TFEB dissociates from 14-3-3 and is able to translocate into the nucleus where it is able to activate transcription of lysosomal genes (28). We therefore assessed the amount of nuclear TFEB as a readout of its activation. The level of nuclear translocation of TFEB was increased upon STAMP2 knockdown, which was further increased upon starvation (Fig. 5B). This is consistent with the increased upregulation of autophagy genes observed upon STAMP2 knockdown in both the RT-qPCR and as well as expression in the human PCa cohort (Fig. 4).
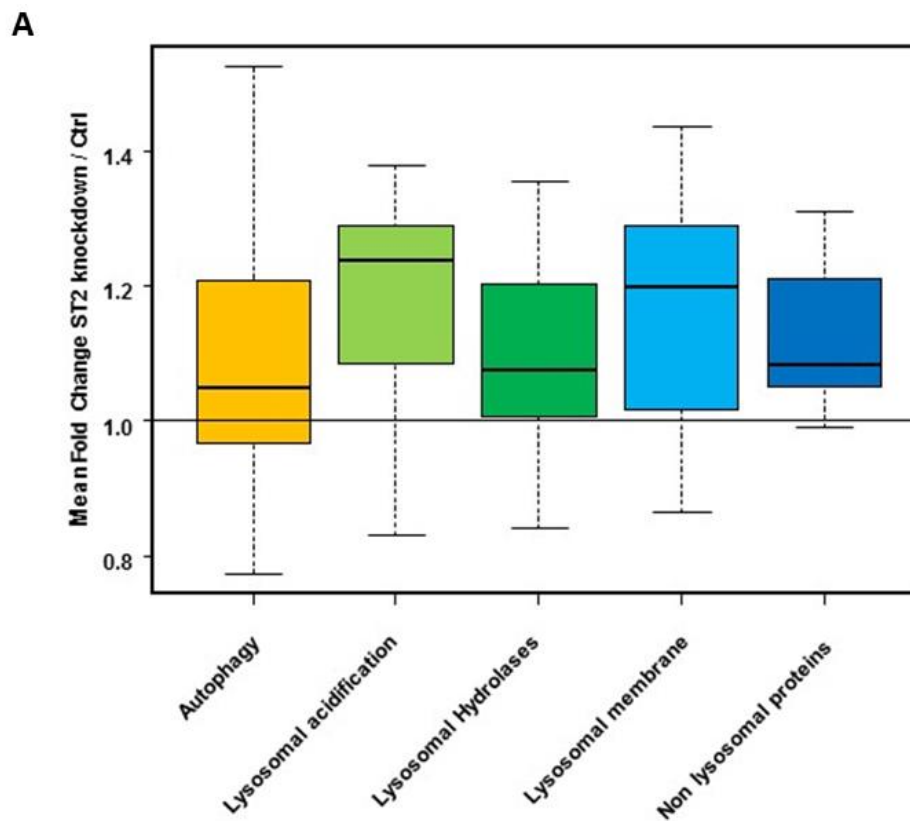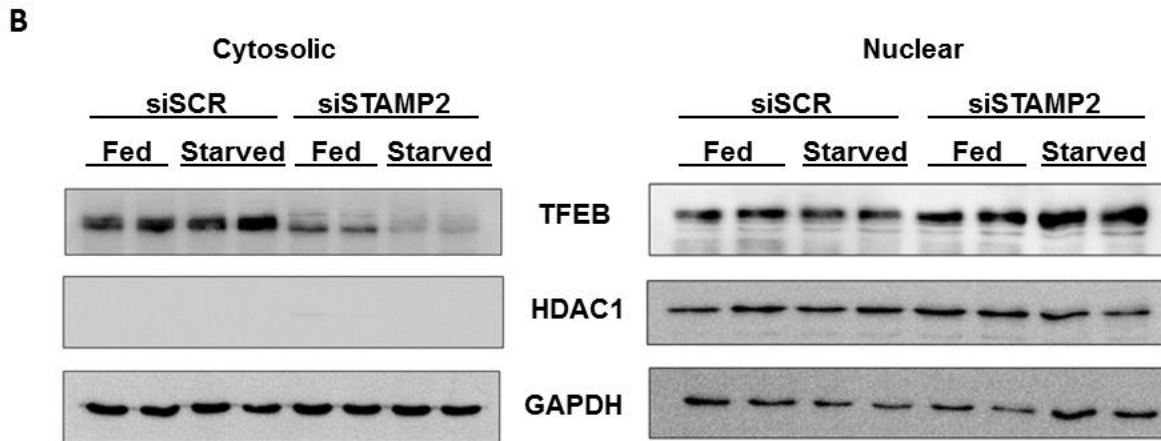
**Figure 5: Nuclear TFEB is increased upon STAMP2 depletion.**

**A**. Gene expression profiles of TFEB target genes in LNCaP siSTAMP2 vs LNCaP control cells determined by cDNA microarray analysis.TFEB target genes were grouped into classes as described in Palmieri et al. (27) **B**. siRNA-treated LNCaP cells were starved or not for 30 minutes in EBSS prior to harvesting cytosolic and nuclear extracts were made and used in western analysis. HDAC1 was used as a control for the nuclear fraction and GAPDH was used as a control for the cytoplasmic fraction.

**STAMP2 knockdown results in increased lysosome number**.

TFEB activation leads to increased lysosomal biogenesis through the upregulation of lysosome related genes (29). To further validate the involvement of TFEB in STAMP2 regulated autophagy, we quantified the amount of lysosomes using lysotracker staining in LNCaP cells. As shown in Fig. 6, STAMP2 siRNA treatment of LNCaP cells resulted in an increase in the lysosome number per nucleus. This increase could be caused by the activation of TFEB, which is known to be involved in lysosomal biogenesis in order to cope with increased degradation by the lysosomes in PCa (30).
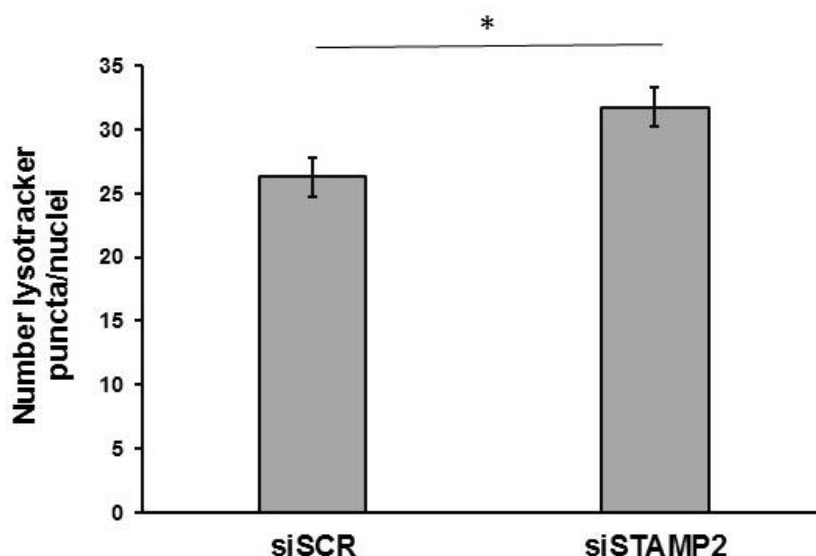


**Figure 6: Lysosome number is increased upon STAMP2 knockdown.**

LNCaP cells were reverse transfected with control or STAMP2 siRNA for 48 hours prior to being loaded with 75 nM lysotracker red for 30 minutes before fixation in 4% PFA (pH 7.2) for 15 minutes and imaging within 24 hours. (* = $p < 0.05$)

# Discussion

Autophagy in PCa promotes cell survival in the face of hormone withdrawal during ADT (13). Therefore, there are multiple clinical trials underway to improve treatment response by simultaneous inhibition of autophagy in PCa. However, currently available autophagy repressors are unspecific and often lead to undesired side effects (31). Thus, identification of new players in autophagy regulation in PCa could open doors to new targets to influence autophagy in PCa cells and may also function as biomarkers to distinguish PCa that are likely to respond to treatment. STAMP2 has been implicated in the development and progression of PCa (18, 21), in part through activation of stress response pathways. However, the role of this transmembrane protein in autophagy remained unclear. Here we show that STAMP2 represses autophagy in PCa, in part through regulation of autophagy gene transcription and post-translational modifications (Fig. 8). The results presented here suggest that STAMP2 is involved in regulating autophagy in PCa.

STAMP2 depletion increases LC3 lipidation (Fig. 1A). However, the lipidation status of the other members of the mammalian Atg8 family homologues, such as GABARAP, -L1, and -L2 remain to be investigated. LC3, but not GABARAP, was shown to be dispensable for bulk autophagy (32). This highlights the need to also include the lipidation status of the GABARAPs in response to manipulation of STAMP2 expression to obtain the full picture of the autophagic flux in PCa. In support of this, *Gabarap*, *-L1*, and *-L2* expression was increased in PCa with low levels of STAMP2 expression (22) (Fig. 4C). Total LC3 (LC3-I and -II) was increased upon STAMP2 knockdown. Transcriptional upregulation or increased processing by ATG4 could possibly cause the increase in LC3-I in STAMP2 knockdown cells. ATG4 processes cytosolic LC3 by cleaving LC3 at the C-terminal to expose a glycine residue necessary for LC3 lipidation (33). As ATG4 protein levels or enzyme kinetics have not been investigated here, the possibility that the observed differences in LC3-I levels stems from increased pre-processing of LC3 cannot be ruled out.

Furthermore, p62 protein levels were not greatly altered upon STAMP2 knockdown, as one might have expected when the autophagic flux is upregulated. This could be due to a technical problem during extraction of p62 from the whole cell. p62 forms aggregates and is often precipitated out in lysis buffers not containing SDS or when spun down at extreme high speeds.

Supplementation of additional SDS to the RIPA lysis buffer will possibly improve the extraction of p62. The co-localization of LC3 and p62 should also be studied to investigate if p62 is indeed being brought into autophagosomes. Furthermore, it would be interesting to investigate the possibility that other autophagy adaptor proteins in addition to p62 may be involved in STAMP2 depletion induced autophagy.

The increase in LLP degradation upon STAMP2 knockdown signifies increased degradation of cytoplasmic material at the lysosomes, an observation that supports the induction of autophagy during STAMP2 depletion. This may be a response towards increased amount of substrates trafficked to the lysosomes through fusion with autophagosomes. However, the contribution of the proteasome in degrading LLP remains to be investigated. Lysosomal inhibition by the use if BafA1 could potentially affect the degradation of substrates at the proteasome (34). As such, incorporating proteasome inhibitors would provide a control to the extent of LLPD degradation by the proteasome.

The ULK complex integrates nutrient signaling through mTOR and AMPK mediated phosphorylation (25). We found that ULK1 phosphorylation on both of its regulatory serine residues affected by mTOR and AMPK was altered upon STAMP2 knockdown. Basal ULK1 phosphorylation at S555 is increased upon STAMP2 knockdown in both LNCaP and VCaP PCa cell lines. This phosphorylation regulates early autophagy events that ultimately lead to recruitment of autophagy proteins to the site of autophagosome formation (35). mTORC1 mediated ULK1 phosphorylation at S757 was almost depleted completely when STAMP2 is knocked down, despite increased mTORC1 activity under these conditions, as shown by increased p70S6K phosphorylation (36). However, previous studies have shown that in certain situations p70S6K activation is not correlated with autophagy activation (37, 38). The changes in ULK1 phosphorylation can possibly be attributed to phosphatases (39) and other Ser/Thr kinases in addition to AMPK and mTOR. These observations indicate that the ULK complex is activated upon the loss of STAMP2, suggesting increased induction of autophagy.

Previous studies in our laboratory showed that STAMP2 induces increased ATF4 expression (21), which is a transcription factor involved in autophagy (40). If ATF4 was the transcription factor involved in mediating the effects of STAMP2 that we observe, we would expect ATF4 levels drop when STAMP2 is knocked down, leading to decreased autophagy gene expression. However, we observed the opposite, whereby the loss of STAMP2 increased *MAP1LC3b* and

*p62* expression, while ectopic expression of STAMP2 decreased the expression of these genes. Even though we did not directly investigate the direct involvement of ATF4 in our experiments, this suggests that a different transcription factor may be involved. Microarray analysis in LNCaP cells showed that TFEB target genes were upregulated upon STAMP2 knockdown (Fig. 5A). Genes involved in lysosome function were found to be increased in STAMP2 knockdown cells and is currently being validated by RT-qPCR. The increase in lysosome gene expression would suggest physiological changes to the lysosomes when STAMP2 is lost. Pathways with endpoints at the lysosomes, such as degradation of endocytosed cell surface receptors (for example, beta-2 adrenergic receptor), should therefore be investigated. Since mTORC1 activation was recently found to be dependent of its recruitment to the lysosomal membrane, changes to lysosomal membrane proteins could explain the increased activation of mTORC1 upon STAMP2 knockdown (41).

Further investigations revealed that upon knockdown of STAMP2, TFEB was predominantly localized in the nucleus (Fig. 5B). Unlike in STAMP2 siRNA treated LNCaP cells, nuclear TFEB was not increased in control cells during the 30 minutes starvation period, indicating enhanced response towards starvation when STAMP2 is depleted. Increasing the amount of time points when the cells are starved would provide increased resolution of the differences in responses towards starvation. Fluorescent-immunolabeling of ectopic TFEB will provide additional validation towards the cell fractionation assay. However, it is important to note that nuclear translocation alone is not proof that TFEB is actively transcribing genes, and further experiments, such as reporter assays are required. The involvement of other transcription factors remain a possibility. Hypoferric conditions induces the stabilization of HIF1a to activate transcription of genes involved in iron homeostasis (42). Preliminary results indicate that HIF1a was not stabilized upon the loss of STAMP2, suggesting that it is not involved in autophagy gene upregulation (data not shown).

The mechanism whereby STAMP2 is able to regulate TFEB translocation is currently being investigated. Given that STAMP2 is an endosomal ferrireductase, its knockdown may lead to accumulation of positively charged iron and copper ions in the endocytic and lysosomal vesicles and may have adverse effects on lysosomal physiology such as lysosomal membrane potential. From the TCGA dataset, we found that the levels of the endolysosomal calcium conducting channel MCOLN1 were inversely correlated to that of STAMP2 (data not shown). MCOLN1 positively regulates TFEB activation through lysosomal calcium release (43) which may also

be regulated by ROS (44), which again is generated by STAMP2 (21).These data indicate that the loss of STAMP2 activates TFEB to induce the expression of autophagy genes, possibly through alterations in cytoplasmic calcium levels. In addition to lysosomal calcium release, TFEB is also regulated by phosphorylation events, by mTORC1, AKT or Glycogen Synthase Kinase (GSK3β) at Ser211 (45), Ser467 (46) and Ser134/138 (47) respectively. Western analysis of phosphorylated TFEB should therefore reveal the kinase(s) that may possibly be involved in its activation upon STAMP2 depletion.

Increased lysotracker puncta staining in STAMP2 siRNA treated cells suggests increased number of lysosomes in the cell. This increase could be caused by the activation of TFEB, which is known to be involved in lysosomal biogenesis in order to cope with increased degradation by the lysosomes in PCa (30). Quantification of lysosome size and lysotracker signal intensity would further reveal more information regarding lysosome fission, regeneration and pH.

Adipocytes treated with antibodies against STAMP2 develop damaged mitochondria (48, 49), indicating a possible role for STAMP2 in maintaining mitochondrial health or removal of damaged mitochondria through mitophagy. Iron depletion induces mitophagy to free up iron stored in the mitochondria (50). Given that iron deficiency phenotypes were observed upon STAMP3 knockdown mice (51), that STAMP2 regulates iron uptake in osteoclasts (20), and STAMP2 depletion attenuates peroxisome proliferator-activated receptor gamma coactivator 1-beta (PGC1β) dependent mitochondrial gene expression (20) it would be interesting to investigate if STAMP2 regulates mitochondrial degradation at the lysosomes. Autophagy adaptor proteins such as OPTN or NBR52 are necessary for mitophagy and their relative protein amounts could therefore serve as early indicators of changes to mitophagy (52). Additionally, mitophagy could be investigated by analysis of mitochondrial DNA and proteins, and mCherry-EGFP-tagged mitochondria.

Tissue culture experiments are often not enough to represent PCa cells in human patients. Signaling events from the surrounding stroma contributes to regulating autophagy (53); as such, the question arises as to whether the increased autophagy in STAMP2 depleted cells are offset or induced in the presence of a functional stroma. To stimulate the physiological conditions of a typical PCa tumor, experiments should eventually be extended to co-culture experiments or *in vivo* systems. Our laboratory has previously reported that STAMP2 knockdown in adipocytes

inhibited adipocyte-facilitated PCa growth in mice (54). The secretion of signaling molecules such as IL-1β and ferritin are mediated by an autophagy-dependent secretory system (55). This raises the possibility that STAMP2 may regulate autophagy, which in turn controls paracrine signaling of secreted cytokines and other proteins.
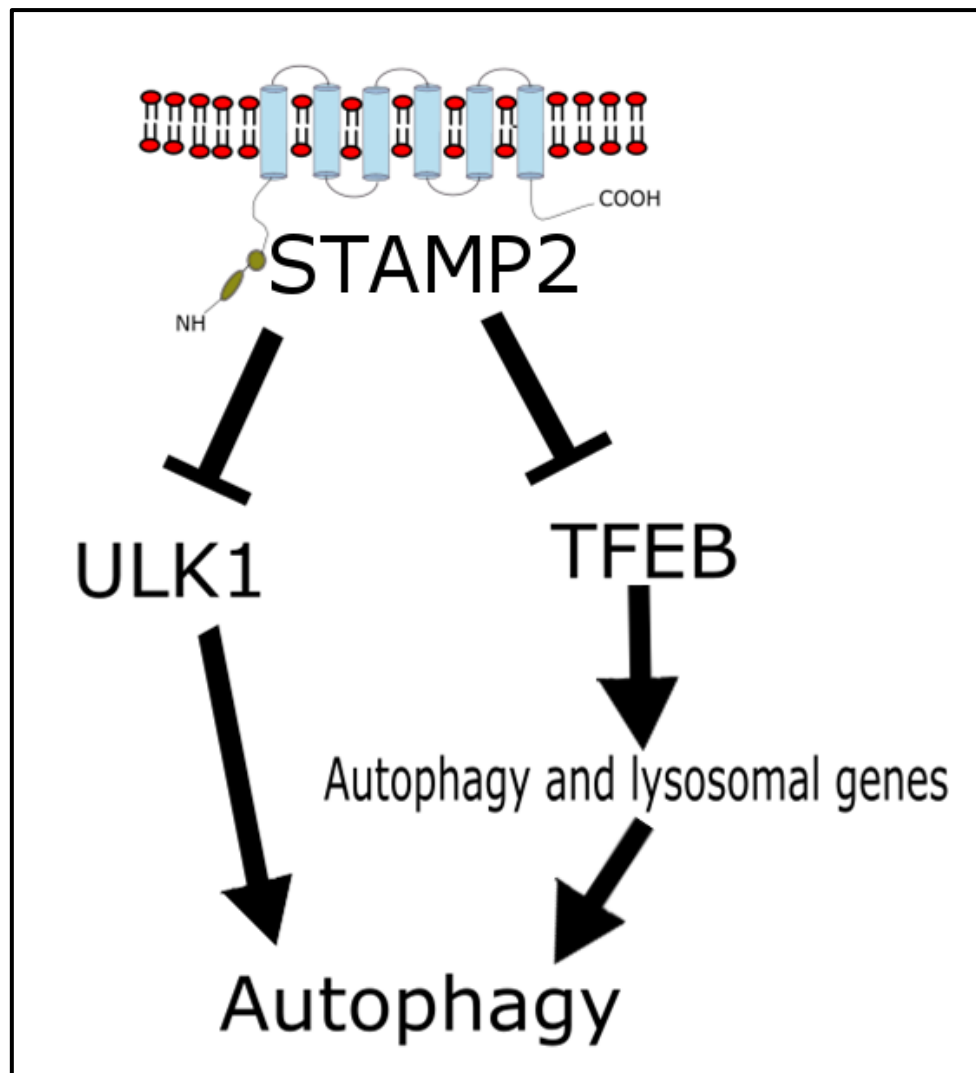


**Figure 8. Graphical summary of the role of STAMP2 in autophagy.**

STAMP2 inhibits the activation of ULK1 and the nuclear translocation of TFEB. This prevents membrane nucleation of the phagophore and expression of autophagy and lysosomal genes, thereby preventing autophagy at different stages of its progression.

STAMP2 expression was previously shown to be androgen responsive (18). Upon depletion of androgens during ADT, STAMP2 levels are greatly reduced; an event that would lead to increased autophagy according to the data presented here. This may contribute to the treatment resistance often observed when cells are faced with ADT (13, 56, 57). The findings presented here warrants further investigations into the relationship between STAMP2 levels and ADT

resistance. In conclusion, we have identified the involvement of STAMP2 in repression of autophagy in PCa through alterations in posttranslational modifications and transcription of autophagy gene. We propose that STAMP2, through mechanisms currently being investigated, inhibit ULK and TFEB activation, thereby repressing autophagy.

# References

1.      Mizushima N, Komatsu M. Autophagy: renovation of cells and tissues. Cell. 2011;147(4):728-41.
2.      White E. The role for autophagy in cancer. The Journal of Clinical Investigation. 2015;125(1):42-6.
3.      Chen N, Karantza V. Autophagy as a therapeutic target in cancer. Cancer biology & therapy. 2011;11(2):157-68.
4.      Lee J, Giordano S, Zhang J. Autophagy, mitochondria and oxidative stress: cross-talk and redox signalling. Biochemical Journal. 2012;441(2):523-40.
5.      Chen S, Zhu X, Qiao H, Ye M, Lai X, Yu S, et al. Protective autophagy promotes the resistance of HER2-positive breast cancer cells to lapatinib. Tumour biology : the journal of the International Society for Oncodevelopmental Biology and Medicine. 2016;37(2):2321-31.
6.      Sun WL, Chen J, Wang YP, Zheng H. Autophagy protects breast cancer cells from epirubicin-induced apoptosis and facilitates epirubicin-resistance development. Autophagy. 2011;7(9):1035-44.
7.      Chen K, Shi W. Autophagy regulates resistance of non-small cell lung cancer cells to paclitaxel. Tumour biology : the journal of the International Society for Oncodevelopmental Biology and Medicine. 2016;37(8):10539-44.
8.      Wu H-M, Jiang Z-F, Ding P-S, Shao L-J, Liu R-Y. Hypoxia-induced autophagy mediates cisplatin resistance in lung cancer cells. Scientific Reports. 2015;5:12291.
9.      Pan H, Wang Z, Jiang L, Sui X, You L, Shou J, et al. Autophagy inhibition sensitizes hepatocellular carcinoma to the multikinase inhibitor linifanib. Scientific Reports. 2014;4:6683.
10.     Kaini RR, Sillerud LO, Zhaorigetu S, Hu C-AA. Autophagy regulates lipolysis and cell survival through lipid droplet degradation in androgen-sensitive prostate cancer cells. The Prostate. 2012;72(13):1412-22.
11.     Jiang Q, Yeh S, Wang X, Xu D, Zhang Q, Wen X, et al. Targeting androgen receptor leads to suppression of prostate cancer via induction of autophagy. The Journal of urology. 2012;188(4):1361-8.
12.     Li M, Jiang X, Liu D, Na Y, Gao GF, Xi Z. Autophagy protects LNCaP cells under androgen deprivation conditions. Autophagy. 2008;4(1):54-60.
13.     Bennett HL, Fleming JT, O'Prey J, Ryan KM, Leung HY. Androgens modulate autophagy and cell death via regulation of the endoplasmic reticulum chaperone glucose-regulated protein 78/BiP in prostate cancer cells. Cell death & disease. 2010;1:e72.
14.     Ferlay J, Soerjomataram I, Dikshit R, Eser S, Mathers C, Rebelo M, et al. Cancer incidence and mortality worldwide: Sources, methods and major patterns in GLOBOCAN 2012. International Journal of Cancer. 2015;136(5):E359-E86.
15.     Uzgare AR, Isaacs JT. Prostate cancer: potential targets of anti-proliferative and apoptotic signaling pathways. Int J Biochem Cell Biol. 2005;37(4):707-14.
16.     Kaini RR, Sillerud LO, Zhaorigetu S, Hu C-AA. Autophagy Regulates Lipolysis and Cell Survival Through Lipid Droplet Degradation in Androgen Sensitive Prostate Cancer Cells. The Prostate. 2012;72(13):1412-22.
17.     Nguyen HG, Yang JC, Kung HJ, Shi XB, Tilki D, Lara PN, Jr., et al. Targeting autophagy overcomes Enzalutamide resistance in castration-resistant prostate cancer cells and improves therapeutic response in a xenograft model. Oncogene. 2014;33(36):4521-30.
18.     Korkmaz CG, Korkmaz KS, Kurys P, Elbi C, Wang L, Klokk TI, et al. Molecular cloning and characterization of STAMP2, an androgen-regulated six transmembrane protein that is overexpressed in prostate cancer. Oncogene. 2005;24(31):4934-45.

19.	Sikkeland J, Saatcioglu F. Differential Expression and Function of Stamp Family Proteins in Adipocyte Differentiation. PLOS ONE. 2013;8(7):e68249.
20.	Zhou J, Ye S, Fujiwara T, Manolagas SC, Zhao H. Steap4 plays a critical role in osteoclastogenesis in vitro by regulating cellular iron/reactive oxygen species (ROS) levels and cAMP response element-binding protein (CREB) activation. J Biol Chem. 2013;288(42):30064-74.
21.	Jin Y, Wang L, Qu S, Sheng X, Kristian A, Maelandsmo GM, et al. STAMP2 increases oxidative stress and is critical for prostate cancer. EMBO molecular medicine. 2015;7(3):315-31.
22.	Abeshouse A, Ahn J, Akbani R, Ally A, Amin S, Andry Christopher D, et al. The Molecular Taxonomy of Primary Prostate Cancer. Cell.163(4):1011-25.
23.	Kabeya Y, Mizushima N, Ueno T, Yamamoto A, Kirisako T, Noda T, et al. LC3, a mammalian homologue of yeast Apg8p, is localized in autophagosome membranes after processing. EMBO J. 2000;19.
24.	Bjorkoy G, Lamark T, Pankiv S, Overvatn A, Brech A, Johansen T. Monitoring autophagic degradation of p62/SQSTM1. Methods in enzymology. 2009;452:181-97.
25.	Kim J, Kundu M, Viollet B, Guan KL. AMPK and mTOR regulate autophagy through direct phosphorylation of Ulk1. Nat Cell Biol. 2011;13(2):132-41.
26.	Abeshouse A, Ahn J, Akbani R, Ally A, Amin S, Andry Christopher D, et al. The Molecular Taxonomy of Primary Prostate Cancer. Cell. 2015;163(4):1011-25.
27.	Palmieri M, Impey S, Kang H, di Ronza A, Pelz C, Sardiello M, et al. Characterization of the CLEAR network reveals an integrated control of cellular clearance pathways. Human molecular genetics. 2011;20(19):3852-66.
28.	Roczniak-Ferguson A, Petit CS, Froehlich F, Qian S, Ky J, Angarola B, et al. The transcription factor TFEB links mTORC1 signaling to transcriptional control of lysosome homeostasis. Science signaling. 2012;5(228):ra42.
29.	Sardiello M, Palmieri M, di Ronza A, Medina DL, Valenza M, Gennarino VA, et al. A gene network regulating lysosomal biogenesis and function. Science (New York, NY). 2009;325(5939):473-7.
30.	Blessing AM, Rajapakshe K, Reddy Bollu L, Shi Y, White MA, Pham AH, et al. Transcriptional regulation of core autophagy and lysosomal genes by the androgen receptor promotes prostate cancer progression. Autophagy. 2017;13(3):506-21.
31.	Farrow JM, Yang JC, Evans CP. Autophagy as a modulator and target in prostate cancer. Nature reviews Urology. 2014;11(9):508-16.
32.	Engedal N, Seglen PO. Autophagy of cytoplasmic bulk cargo does not require LC3. Autophagy. 2016;12(2):439-41.
33.	Satoo K, Noda NN, Kumeta H, Fujioka Y, Mizushima N, Ohsumi Y, et al. The structure of Atg4B–LC3 complex reveals the mechanism of LC3 processing and delipidation during autophagy. The EMBO Journal. 2009;28(9):1341-50.
34.	Korolchuk VI, Mansilla A, Menzies FM, Rubinsztein DC. Autophagy Inhibition Compromises Degradation of Ubiquitin-Proteasome Pathway Substrates. Molecular Cell. 2009;33(4):517-27.
35.	Egan DF, Kim J, Shaw RJ, Guan K-L. The autophagy initiating kinase ULK1 is regulated via opposing phosphorylation by AMPK and mTOR. Autophagy. 2011;7(6):645-6.
36.	Banerjee P, Ahmad MF, Grove JR, Kozlosky C, Price DJ, Avruch J. Molecular structure of a major insulin/mitogen-activated 70-kDa S6 protein kinase. Proceedings of the National Academy of Sciences of the United States of America. 1990;87(21):8550-4.
37.	Datan E, Shirazian A, Benjamin S, Matassov D, Tinari A, Malorni W, et al. mTOR/p70S6K signaling distinguishes routine, maintenance-level autophagy from autophagic cell death during influenza A infection. Virology. 2014;452–453:175-90.

38.	Ci Y, Shi K, An J, Yang Y, Hui K, Wu P, et al. ROS inhibit autophagy by downregulating ULK1 mediated by the phosphorylation of p53 in selenite-treated NB4 cells. Cell death & disease. 2014;5:e1542.

39.	Torii S, Yoshida T, Arakawa S, Honda S, Nakanishi A, Shimizu S. Identification of PPM1D as an essential Ulk1 phosphatase for genotoxic stress-induced autophagy. EMBO reports. 2016.

40.	B'Chir W, Maurin AC, Carraro V, Averous J, Jousse C, Muranishi Y, et al. The eIF2alpha/ATF4 pathway is essential for stress-induced autophagy gene expression. Nucleic acids research. 2013;41(16):7683-99.

41.	Sancak Y, Bar-Peled L, Zoncu R, Markhard AL, Nada S, Sabatini DM. Ragulator-Rag complex targets mTORC1 to the lysosomal surface and is necessary for its activation by amino acids. Cell. 2010;141(2):290-303.

42.	Peyssonnaux C, Nizet V, Johnson RS. Role of the hypoxia inducible factors HIF in iron metabolism. Cell cycle (Georgetown, Tex). 2008;7(1):28-32.

43.	Medina DL, Di Paola S, Peluso I, Armani A, De Stefani D, Venditti R, et al. Lysosomal calcium signalling regulates autophagy through calcineurin and TFEB. Nat Cell Biol. 2015;17(3):288-99.

44.	Zhang X, Cheng X, Yu L, Yang J, Calvo R, Patnaik S, et al. MCOLN1 is a ROS sensor in lysosomes that regulates autophagy. Nature Communications. 2016;7:12109.

45.	Martina JA, Chen Y, Gucek M, Puertollano R. MTORC1 functions as a transcriptional regulator of autophagy by preventing nuclear transport of TFEB. Autophagy. 2012;8(6):903-14.

46.	Palmieri M, Pal R, Nelvagal HR, Lotfi P, Stinnett GR, Seymour ML, et al. mTORC1-independent TFEB activation via Akt inhibition promotes cellular clearance in neurodegenerative storage diseases. Nature Communications. 2017;8:14338.

47.	Li Y, Xu M, Ding X, Yan C, Song Z, Chen L, et al. Protein kinase C controls lysosome biogenesis independently of mTORC1. Nat Cell Biol. 2016;18(10):1065-77.

48.	Qin DN, Zhu JG, Ji CB, Chunmei S, Kou CZ, Zhu GZ, et al. Monoclonal antibody to six transmembrane epithelial antigen of prostate-4 influences insulin sensitivity by attenuating phosphorylation of P13K (P85) and Akt: possible mitochondrial mechanism. Journal of bioenergetics and biomembranes. 2011;43(3):247-55.

49.	Qin DN, Kou CZ, Ni YH, Zhang CM, Zhu JG, Zhu C, et al. Monoclonal antibody to the six-transmembrane epithelial antigen of prostate 4 promotes apoptosis and inhibits proliferation and glucose uptake in human adipocytes. International journal of molecular medicine. 2010;26(6):803-11.

50.	Allen GFG, Toth R, James J, Ganley IG. Loss of iron triggers PINK1/Parkin-independent mitophagy. EMBO reports. 2013;14(12):1127-35.

51.	Zhang F, Tao Y, Zhang Z, Guo X, An P, Shen Y, et al. Metalloreductase Steap3 coordinates the regulation of iron homeostasis and inflammatory responses. Haematologica. 2012;97(12):1826-35.

52.	Lazarou M, Sliter DA, Kane LA, Sarraf SA, Wang C, Burman JL, et al. The ubiquitin kinase PINK1 recruits autophagy receptors to induce mitophagy. Nature. 2015;524(7565):309-14.

53.	Maes H, Rubio N, Garg AD, Agostinis P. Autophagy: shaping the tumor microenvironment and therapeutic response. Trends in Molecular Medicine.19(7):428-46.

54.	Lindstad T, Qu S, Sikkeland J, Jin Y, Kristian A, Maelandsmo GM, et al. STAMP2 is required for human adipose-derived stem cell differentiation and adipocyte-facilitated prostate cancer growth in vivo. Oncotarget. 2016.

55.	Kimura T, Jia J, Kumar S, Choi SW, Gu Y, Mudd M, et al. Dedicated SNAREs and specialized TRIM cargo receptors mediate secretory autophagy. The EMBO Journal. 2016.

56. Bennett HL, Stockley J, Fleming JT, Mandal R, O'Prey J, Ryan KM, et al. Does androgen-ablation therapy (AAT) associated autophagy have a pro-survival effect in LNCaP human prostate cancer cells? BJU international. 2013;111(4):672-82.

57. Karantanos T, Corn PG, Thompson TC. Prostate cancer progression after androgen deprivation therapy: mechanisms of castrate resistance and novel therapeutic approaches. Oncogene. 2013;32(49):5501-11.